Thesis for the Degree of Master of Engineering

Optimization of Phenolic Compounds in Subcritical Water Extracts from *Ecklonia stolonifera* by Response Surface Methodology

by

Ye-Seul Park

Department of Food Science and Technology

The Graduate School

Pukyong National University

February 2024

Optimization of Phenolic Compounds in Subcritical Water Extracts from *Ecklonia stolonifera* by Response Surface Methodology

반응표면법에 의한 곰피(*Ecklonia stolonifera*) 아임계 수 추출물의 페놀 화합물 최적화

Advisor: Prof. Byung-Soo Chun

by

Ye-Seul Park

A thesis submitted in partial fulfillment of the requirements for the degree of

Master of Engineering

in Department of Food Science and Technology, The Graduate School,
Pukyong National University

February 2024

Optimization of Phenolic Compounds in Subcritical Water Extracts from *Ecklonia stolonifera* by Response Surface Methodology

A dissertation

by

Ye-Seul Park

Approved by:

_____

Dong-Hyun Ahn, Ph.D.
(Chairman)

_____

Yang-Bong Lee, Ph.D.
(Member)

_____

Byung-Soo Chun, Ph.D.
(Member)

February 16, 2024

Contents

List of Tables

List of Figures

Optimization of Phenolic Compounds in Subcritical Water Extracts from *Ecklonia stolonifera* by Response Surface Methodology

Ye-Seul Park

Department of Food Science and Technology, The Graduate School,

Pukyong National University

Abstract

Ecklonia stolonifera is a type of seaweed that belongs to the kelp family Seaweedaceae. Several studies have demonstrated its bioactive compounds. To extract these compounds, critical water hydrolysis was used, which is a green extraction technique. The reaction temperature of hydrolysis ranged from 120℃ to 220℃, and it played a crucial role in releasing active compounds such as sugars, phenols, flavonoids, and antioxidants. The results of temperature specific extraction indicate that the optimal temperature condition is 195℃. Therefore, we set the center temperature of the response surface methodology (RSM) at 195℃, and varied the temperature between 160℃, 195℃, and 230℃, the time between 20min, 40min, and 60min, and the ratio between 10 g/mL, 20 g/mL, and 30 g/mL. The optimal conditions for extraction temperature, time, and ratio were found to be 198.50℃, 36.21 min, and 12.23 g/mL. The individual phenolic compounds in the extract were identified using high-performance liquid chromatography (HPLC). The predominant phenolic compounds found were 4-hydroxybenzoic acid, chlorogenic acid, rutin, gallic acid, and 4-hydroxy-3,5-dimethoxycinnamic acid. *E. stolonifera* subcritical water extract exhibited high antioxidant activity in various assays, including $ABTS^+$, DPPH, and FRAP. Under optimal conditions, the $ABTS^+$ value was 70.94 ± 0.15 mg trolox equivalent/g dried sample, the DPPH value was 60.03 ± 0.35 mg trolox equivalent/g dried sample, and the FRAP value was 29.45 ± 0.39 mg trolox equivalent/g dried sample. These values were higher than those of the ethanol extract. Additionally, the physicochemical properties of *E. stolonifera* were analyzed, including TPC, TFC, TSC, and RSC. The TPC value for the optimal

condition extract was 50.01 ± 0.12 mg phloroglucinol/g dried sample, and the TFC value was 43.58 ± 0.01 mg quercetin equivalent/g dried sample, which were approximately three times higher than the total phenolic content of the ethanol extract. The TSC and RSC values were higher in the ethanol extract, with 55.06 ± 1.51 mg glucose/g dried sample and 19.22 ± 0.23 mg glucose/g dried sample, respectively. The structural characterization (XRD, FT-IR) was also compared with the raw powder. The XRD analysis indicated high levels of KCl in the raw powder, while NaCl was predominantly observed in OCE-ES and ethanol extracts. The FT-IR analysis showed the presence of O-H, C-H, -C≡C-, O-C-O, and C-O groups in all three extracts. In the evaluation of antihypertensive activity, the positive control of 1% Captopril showed an activity of ≤99.22% ± 0.01%, while OCE-ES showed a higher activity of ≤95.87% ± 0.01% at a concentration of only 0.5%. Regarding anti-diabetic activity, the positive control of 1% acarbose showed ≤96.68% ± 0.07% activity, while OCE-ES showed ≤69.29% ± 1.83% activity and the ethanol extract showed ≤92.67% ± 1.13% activity. To test for anti-inflammatory activity, a positive control of 1% Diclofenac sodium was used and showed an activity of ≤66.80% ± 0.84%. OCE-ES showed an activity of ≤68.55% ± 0.98%, while the ethanol extract showed an activity of ≤41.62% ± 0.66%. This study utilized the subcritical water extraction method to determine the bioactivity of *E. stolonifera* extracts and confirmed their potential as a functional food material. Furthermore, these extracts can be applied to various industrial field.

I. Introduction

Ecklonia stolonifera is a type of seaweed belonging to the kelp family Lessoniaceae. It grows on the southern coast of Korea, the southern east coast, Ulleungdo Island, and Dokdo Island, as well as in Japan. The stem of the plant measures between 10 and 25 cm in length and is characterized by two irregularly arranged layers of mucilage. The leaves are broad, measuring from 30 cm to 1 m in length and are serrated along the edges. The plant produces mucilage in November, which fully develops by the following autumn (NIFS, 2023). A previous study confirms that *E. stolonifera* extract has a high concentration of phenolic compounds and demonstrates bioactivity, including liver protection, anti-inflammatory effects and antioxidant properties due to the presence of phenolic compounds (Jung et al., 2014b). Additionally, *E. stolonifera* has been found to have hepatoprotective effects against hepatotoxicity (Jung et al., 2014b), anti-obesity activity on adipocytes (Jung et al., 2014a) and anti-diabetic properties through fucosterol (Jung et al., 2013). Studies have shown that *E. stolonifera* has antioxidant and antibacterial properties (Kuda et al., 2007) and anti-inflammatory properties through phlorotannins (Kim et al., 2009; Lee et al., 2012; Wei et al., 2016). The development of an anti-photoaging agent using *E. stolonifera* extract was also explored. Joe M. J. (2006) conducted a study on the anti-dementia activity of sterols and phlorotannins in *E. stolonifera* (Joe et al., 2006). Yoon N. Y. (2008) evaluated the antihypertensive activity of phlorotannins in the same plant (Yoon et al., 2008). Furthermore, Jung H. A. (2006) investigated its potential as a treatment for hypertension (Jung et al., 2006). Men X. (2022) analyzed the bioactive compounds extracted from *E. stolonifera* (Men

et al., 2022). Several studies have investigated the functions of bioactive compounds extracted from *E. stolonifera*, including their effects (Kang et al., 2004). Although *E. stolonifera* contains physiologically and functionally active compounds, it is more commonly used as feed for complex fish farms than as a therapeutic agent.

Phlorotannins are polyphenolic compounds formed through the polymerization of monomeric units. They are biosynthesized using the acetate-malonate pathway (Li et al., 2011). Phlorotannins are categorized into four types based on the bonding method: fuhalol and phloretol with ether bonds, fucole with phenyl bonds, fuco-phloroeckol with ether and phenyl bonds and eckol with ether bonds (Li et al., 2011). Previous studies have shown that phenolic compounds, particularly phlorotannins, possess anti-bacterial properties (Nagayama et al., 2002). Phlorotannins have been investigated for their potential as anti-SARS drugs against viruses caused by SARS-CoV infection (Park et al, 2013). Additionally, Sansone (2020) presented the antiviral function of phlorotannins, as well as their antioxidant, anti-inflammatory and anti-MRSA qualities, which Nair (2019) also emphasized (Sansone et al., 2020; Nair et al., 2019). Shrestha (2021) noted the potential of this functional food ingredient in the domains of anti-inflammatory and neuroprotective activities. It is widely acknowledged that this ingredient holds great promise for the creation of treatment and prevention products due to its bioactive properties, which include anti-diabetic and anti-cancer effects (Jung et al, 2014a; Khan et al., 2022; Meng et al., 2021; Ryu et al., 2009).

Table 1. Scientific classification of *Ecklonia stolonifera*

Scientific classification	
Kingdom	Chromista
Phylum	Ochrophyta
Class	Phaeophyceae
Order	Laminariales
Family	Lessoniaceae
Genus	*Ecklonia*
Species	***E. stolonifera***

Figure 1. A picture of *E. stolonifera*

Water reaches its critical state at pressures of 22 MPa and temperatures ranging from 100℃ to 374℃ (figure 2). In this state, it can be used as an extraction medium due to its high hydrolysis capacity and dielectric constant similarity with organic solvents (Park et al., 2023b). The use of traditional organic solvents, such as methanol and ethanol, is not only time-consuming but also harmful to human health due to their solvent properties. Subcritical water extraction uses water as a safe solvent, making it more suitable for separating food constituents (Cheng et al., 2021). Temperature is one of the key factors affecting supercritical water extraction, as it reduces the dielectric constant and increases the diffusion rate as the temperature rises (Asl & Khajenoori, 2013). According to Gbashi S. (2017), increasing the pressure during extraction can improve water penetration into areas that are not accessible under atmospheric pressure, thereby increasing the extraction force (Gbashi et al., 2017).

Response surface methodology (RSM) is a statistical technique that fits a polynomial equation to experimental data using multivariate statistical techniques to determine the optimum extraction conditions for a variable by altering several variables. Two RSM methods exist: central composite design (CCD) and Box-Behnken design (BBD). The BBD is commonly used in response surface methodology experiments. The BBD is a quadratic design that consists of three variables. It can rotate and is based on a nearly spherical space, as referenced by Lou H. (2013) and Saravana P. S. (2019) (Lou et al., 2013; Saravana et al., 2019). The variables are all within a distinct area, which reduces errors, as detailed by Oyinade A. (2016) (Oyinade et al., 2016). One major benefit of using BBD is its ability to examine multiple parameters with fewer experiments compared to other statistical techniques, as noted by Alhajabdalla M. (2021) (Alhajabdalla et al., 2021).

In this study, bioactive compounds were extracted from *E. stolonifera* using the clean process technique of subcritical water extraction. The optimised conditions were found using the BBD of RSM. The compounds were characterised by analysing their phenolic content, sugar content, antioxidant, antihypertensive, antidiabetic, anti-inflammatory activities, and structural properties.

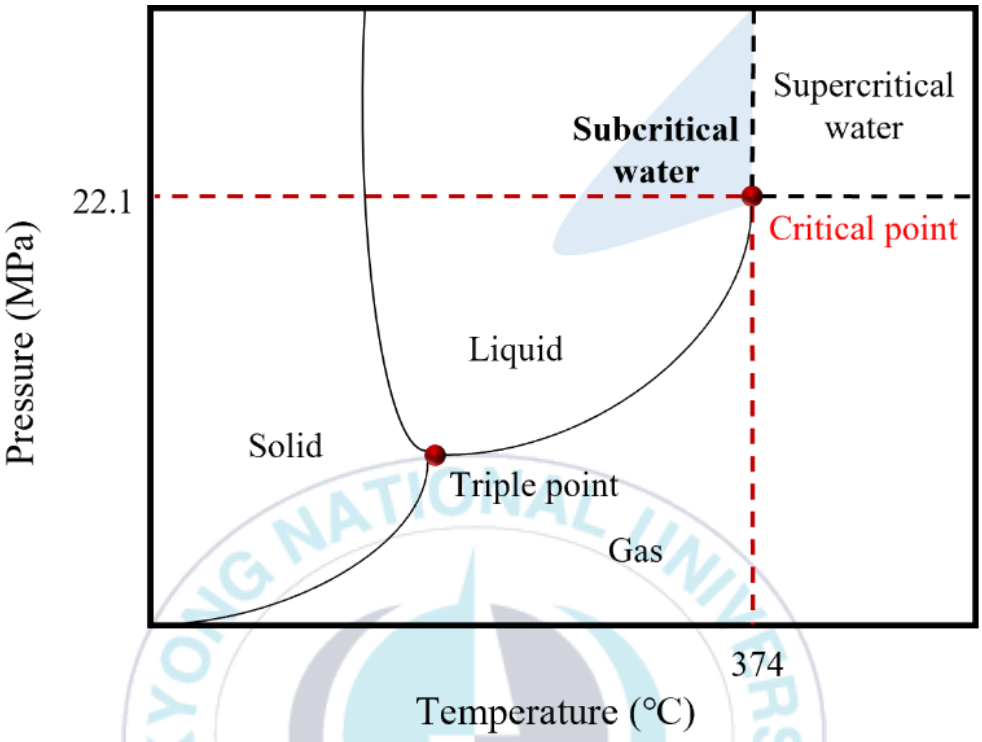

Figure 2. Physical state of water at different temperature and pressure

II. Materials and Methods

1. Chemical reagent

Ecklonia Stolonifera used in this experiment was obtained from Deundeun Bada Co., Ltd. located in Gijang-gun, Busan and subjected to freeze-drying at -80℃ for 72 hr using a HyperCOOL HC8080 (BMS Co., Ltd., Korea). After drying, the sample was ground in a PN SMKA-4000 mixer (PN Co., Ltd., Korea), passed through a 710 μm sieve, and stored at -60℃ before being used in subsequent experiments. The high-purity nitrogen gas used for subcritical water extraction was obtained from KOSEM in Yangsan, Korea. The standard materials and HPLC grade reagents used in the experiment were provided by Samjeon Pure Chemical Co., Ltd. in Gyeonggi, Republic of Korea. Sep-Pak C18 cartridges were purchased from Thermo Scientific™.

2. Experimental method

2.1. Proximate composition analysis of *E. stolonifera*

The general components of the freeze-dried sample were analyzed following the AOAC (2000) standard method (AOAC, 2000). Moisture content was determined us-

ing the atmospheric heat drying method, ash content was assessed through the dry incineration process, crude protein concentration was measured using the Kjeldahl technique, and crude fat content was determined using the Soxhlet method. The total carbohydrate content was calculated by subtracting the sum of moisture, ash, crude protein, and crude fat from 100. Abbreviations were defined upon their initial usage.

The moisture content of the sample was determined by drying it at 105℃ under regular pressure for 3-5 hr. The resulting decrease in weight indicated the amount of moisture present. A preheated weighing dish was used to hold 5 g of the sample. After drying, the sample was cooled in a desiccator for approximately 30 min before being weighed. The moisture content was calculated using the provided formula, 1.

$$\frac{b-c}{b-a} \times 100\ (\%) \cdots\cdots\cdots\cdots\cdots\cdots\cdots\cdots\cdots\cdots (1)$$

a: Mass of weighing dish (g)

b: Mass of weighing dish and sample (g)

c: Mass at constant weight after drying (g)

The ash was produced using the dry incineration method. The sample was placed in a crucible and heated to a temperature between 550 and 600℃ until it was completely incinerated. 1 g of the powdered sample was then heated in a preheated furnace at 550℃ until it turned white or off-white. After the heating process was completed, the sample was transferred to a desiccator and left to cool for about 30 min. It was ensured that the temperature dropped below 200℃ before weighing. The quantity of the sample was then calculated using the provided formula, 2.

$$\frac{W_1 - W_0}{S} \times 100\ (\%) \cdots\cdots\cdots\cdots\cdots\cdots\cdots\cdots (2)$$

W_0: Mass of the crucible with constant mass (g)

W_1: Mass of crucible and ash after incineration (g)

S: Sample collection amount (g)

Crude protein was extracted by the Kjeldahl method. For this, 1 g of the powdered sample, decomposition accelerator ($CuSO_4$:K_2SO_4, 1:4), and 20 mL of concentrated sulfuric acid were added to the Kjeldahl flask. The analysis was carried out using a digestion unit (K-425, Buchi), followed by a Kjelflex K-360 distillation unit and a titration unit. The sample was analyzed using the 848 Titrino plus Metrohm. The crude protein content (%) was determined by multiplying it by the nitrogen coefficient of 6.25.

Crude fat analysis was performed using the Soxhlet method. A cylindrical filter containing 5 g of the powdered sample was inserted into the extraction tube of the Soxhlet extraction device, covered with cotton wool, and extracted for 24 hr using n-Hexane as a solvent. The extraction device used was the Premium Analog Multi Heating Mantles from DAIHAN-Scientific in Korea. After the extraction process, we used a rotary evaporator (Eyela N-110, Rikakikai, China) to remove the solvent. We then transferred the resulting product to a data container, cooled it for approximately 30 min, and weighed it. We calculated the crude fat concentration of the specimen using the provided formula, 3.

$$\frac{W_1 - W_2}{W} \times 100(\%) \cdots\cdots\cdots\cdots\cdots\cdots\cdots\cdots (3)$$

W_1: Weight of lipid and flask (g)

W_2: Clean flask after drying (g)

W: Weight of initial sample (g)

2.2. Subcritical water extraction

E. stolonifera hydrolysate was obtained using a high-temperature, high-pressure reactor with a volume of 1000 cm^3 made of special metal Hastelloy C276, and a subcritical water hydrolysis apparatus with electric heating, cooling, and stirring components (Figure 3). 30 g of the powder sample and 600 mL of distilled water (w/v, 1:20) were introduced using nitrogen gas at an initial pressure of 30 bar. The stirring speed was set to 200 rpm, and the reaction was carried out at experimental temperatures ranging from 120 to 220℃ for 30 min. Afterward, the resulting hydrolysate was filtered through Chmlab Group F1091-110 filter paper, and the residue was dried to determine the hydrolysis efficiency. The efficiency was calculated using the following formula, 4.

$$\text{Hydrolysis efficiency (\%)} = \frac{\text{amount of sample (g)} - \text{amount of residue after hydrolysis (g)}}{\text{amount of sample (g)}} \cdots\cdots\cdots\cdots (4)$$

For the comparative experiment, 30 g of the powdered sample were combined with 600 mL of methanol solvent (w/v, 1:20). The mixture was then subjected to a 72 hr reaction at 25℃ using a magnetic stirrer set at a stirring speed of 200 rpm. After the

reaction, the resulting residue was filtered through filter paper (Chmlab Group, F1091-110), dried and the hydrolysis efficiency was calculated. The residue was stored at 4℃ until it was utilized in subsequent experiments.

2.3. Experimental design using response surface methodology (RSM)

Response surface analysis was used to optimize the polyphenol content of *E. stolonifera*. The experimental plan chosen was a BBD that included three independent variables: extraction temperature (X_1, ranging from 120 to 220℃), extraction time (X_2, ranging from 20 to 60 min), and solid-to-liquid ratio during extraction (X_3, ranging from 10 to 30 g/mL). The experimental design, which utilized the Box-Behnken methodology, consisted of 17 experiments, including 12 axial points and 5 central points. The dependent variable was the total polyphenol content (Y, mg PG/DW). Regression analysis was performed using the average value from three repeated experiments. The Design Expert statistical software (Version 7.1.0, USA) was used to execute the experimental design and the resulting quadratic equation is presented below (5).

$$Y = \beta_0 + \sum_{i=1}^{3} \beta_i X_i + \sum_{i=1}^{3} \beta_{ii} X_i^2 + \sum \sum_{i<j=1}^{3} \beta_{ii} X_i X_j \cdots\cdots\cdots (5)$$

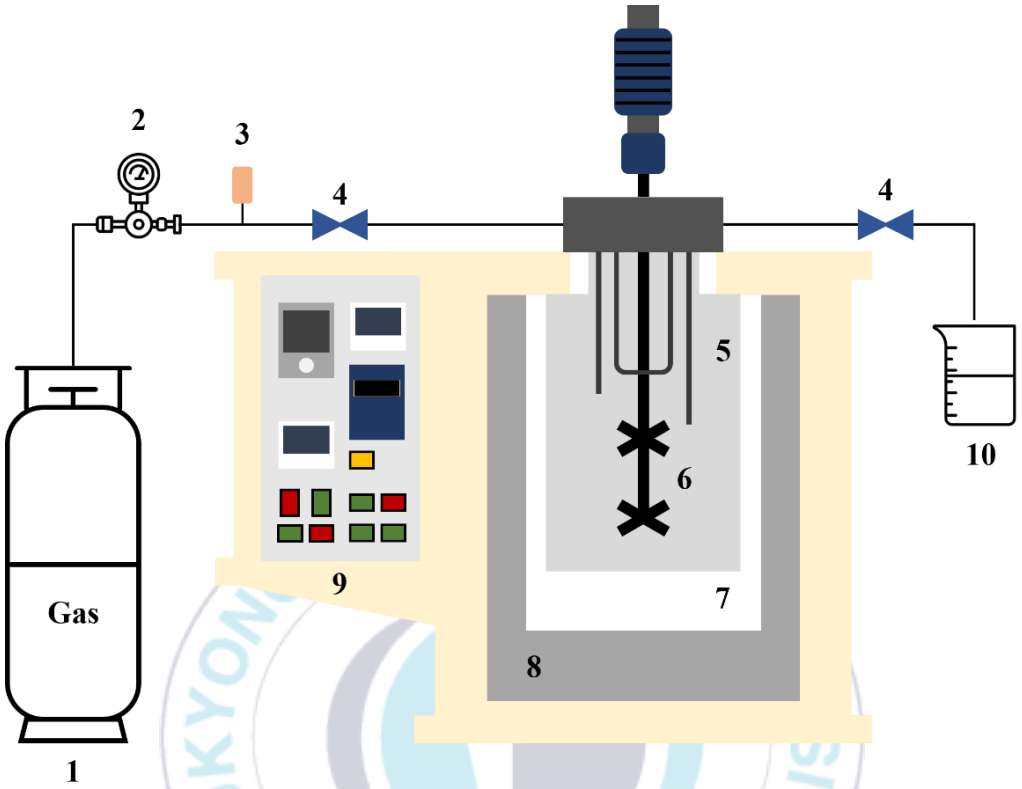

Figure 3. Schematic diagram of the subcritical water hydrolysis apparatus

2.4. Analysis of phenolic compounds using high performance liquid chromatography (HPLC)

Park's (2022) method was used to analyze hydrolyzed phenolic compounds extracted through subcritical water (Park et al., 2022). The resulting hydrolysate was filtered using a hydrophilic membrane filter with a pore size of 0.20 μm. The HPLC system used in the analysis consisted of a Jasco PU-2089 pump, Jasco CO-2060 column oven, and a Jasco UV-2075 UV/VIS detector, all manufactured by Jasco Inc. in Tokyo, Japan. The HPLC analysis was performed using water, formic acid, and acetonitrile solvents in the mobile phase. A YMC-Triart C18 column (4.6 mm x 250 mm, 5 μm) was used. The standard material for each phenol compound was diluted to concentrations of 1, 2.5, 5, 10, 25, and 50 ppm. A calibration curve was established, and the phenol compound content in the hydrolysate was expressed in mg/g of dried sample.

To analyze phenolic compounds in the optimal extract, we employed Sep-Pak Cl8 cartridges as a pretreatment method. Firstly, the Sep-Pak Cl8 cartridge was activated by sequentially passing 6 mL of methanol, 6 mL of water, and 3 mL of the sample. Subsequently, phenolic compounds were eluted by passing 6 mL of water/acetonitrile (85:15) through the cartridge, and the eluate was collected in a vial. The water/acetonitrile ratio (85:15) matches the mobile phase solvent utilized in HPLC analysis, which consists of 1% phosphoric acid in water (solvent A), and 1% phosphoric acid in acetonitrile (solvent B).

2.5. Maillard reaction products (MRPs)

Hydrolysate of *E. stolonifera* was analyzed for Maillard reaction products under optimum extraction conditions using Pangestuti's method (Pangestuti et al., 2021). The degree of browning was measured by determining the absorbance at wavelengths of 294 and 420 nm with a Synergy HT microplate reader (BioTek Instruments, Winooski, VA, USA). The absorbance ratio (A294/A490) was then calculated to determine the degree of browning under ultraviolet light. It was confirmed that the absorbent compound had transformed into a brown polymer.

2.6. Heavy metal

Heavy metal contents of the *E. stolonifera* hydrolysate were measured using an inductively coupled plasma mass spectrometer (PerkinElmer/NexION 300D). The method was slightly modified from that of Čmiková N. (2022) to ensure accurate measurements (Čmiková et al., 2022).

2.7. Analysis of physical properties

2.7.1. pH

pH of the hydrolyzed *E. stolonifera* was determined using a pH meter (Thermo Scientific, ORION STAR A211, Waltham, MA, USA). Before measurement, standardization was conducted by correction with pH buffer solutions (pH 1, pH 4, pH 7, and pH 10).

2.7.2. Color

Color of the hydrolysate from *E. stolonifera* was measured using a colorimeter (Lovibond RT series, The Tintometer Ltd, Amesbury, USA). The results were presented as three-dimensional coordinates in the L^*, a^*, b^* color space, where L^* corresponds to lightness (100), a* represents red ($+a^*$) and green ($-a^*$), and b* represents yellow ($+b^*$) and blue ($-b^*$).

2.7.3. Fourier-transform infrared spectroscopy (FT-IR)

FTIR spectrum was obtained by lyophilizing the hydrolysate and comparing it with the raw powder. Molecular structural changes were detected in the range of 4000-500 cm^{-1} using an infrared spectrometer (FTIR, JASCO, FT-4100).

2.7.4. X-Ray diffraction analysis (XRD)

The hydrolysate was lyophilized for comparison with the raw sample before conducting XRD analysis, which confirmed the presence of crystallinity in the range of 5-80° using a Rigaku/UltimaIV X-ray diffractometer.

2.8. Analysis of antioxidant activity

2.8.1. $ABTS^+$ radical scavenging

$ABTS^+$ radical scavenging capacity of the hydrolysate from *E. stolonifera* and extracts obtained using organic solvents was assessed according to the method described by Haq M. (2017) (Haq et al., 2017) with minor adjustments. First, an $ABTS^+$ solution was created by combining a 7 mM aqueous $ABTS^+$ solution with a 2.45 mM aqueous potassium persulfate solution and allowing it to react for 12 hr in the dark. The $ABTS^+$ solution was then diluted using methanol to obtain an absorbance of 0.70 ± 0.02. A mixture containing 100 μL of hydrolysate and 3.9 mL of $ABTS^+$ solution was vortexed for 10 sec before being allowed to react in the dark for 6 min. Technical abbreviations were defined when first mentioned. Following this, a spectrophotometer (BioTek Instruments, Winooski, VT, USA) was used to measure absorbance in triplicate at 734 nm. Trolox (Sigma Chemical Co., USA) was used as the standard, and after calibration ($y=-0.0012x+0.6445$, $R^2=0.9948$), the antioxidant content of the hydrolysate and organic solvent extract was reported as mg trolox equivalent/g dried sample.

2.8.2. DPPH radical scavenging

DPPH radical scavenging ability of *E. stolonifera*'s hydrolysate and organic solvent extract was evaluated by modifying the approach outlined by Haq M. (2017) (Haq et al., 2017). The process entailed adding 100 μL of hydrolysate to 3.9 mL of DPPH solution (0.00394 g/100 mL of methanol), followed by vortexing for 10 sec and allowing it to react in the dark for 30 min. The absorbance was measured thrice at 517 nm using a spectrophotometer (BioTek Instruments, Winooski, VT, USA). Trolox (Sigma Chemical Co., USA) was used as the standard for quantifying the antioxidant content of the hydrolysate and organic solvent extract in mg trolox equivalent/g dried sample. This was done by constructing a calibration curve ($y=-0.0009x+0.5074$, $R^2=0.9918$).

2.8.3. Ferric reducing antioxidant power (FRAP)

Iron ion reduction capacity of the *E. stolonifera* hydrolysate and organic solvent extract was measured with minor modifications to Gereniu's method described in 2017 (Gereniu et al., 2017). The FRAP solution was prepared by mixing a 300 mM acetate buffer, TPTZ (10 mM TPTZ in 40 mM HCl), and ferric chloride (20 mM ferric chloride) in a ratio of 10:1:1 (v/v). Next, 0.3 mL of the hydrolysate and 3 mL of the FRAP solution were combined, vortexed for 10 sec, and then allowed to react in the dark for 4 min. The absorbance was measured three times at 593 nm utilizing a spectrophotometer (BioTek Instruments, Winooski, VT, USA). Trolox (Sigma Chemical Co., USA) was

utilized as the standard substance. After creating the calibration curve ($y=0.0075x+0.1567$, $R^2=0.9971$), the antioxidant levels of the hydrolysate and organic solvent extract were expressed as mg trolox equivalent/g of dried sample.

2.9. Analysis of phenol content

2.9.1. Total phenolic content (TPC)

To quantify the total phenolic content of the *E. stolonifera* hydrolysate and organic solvent extract, we mixed 1 mL of the hydrolysate, 1 mL of Folin-Ciocalteu reagent (in a 1:10 ratio), and 0.8 mL of 7.5% sodium carbonate solution. After vortexing for 10 sec, the mixture was allowed to react for 2 hr in the absence of light. Using a spectrophotometer (BioTek Instruments, Winooski, VT, USA), we measured absorbance three times at 765 nm. The standard used for this study was phloroglucinol (Sigma Chemical Co., USA). To determine the total phenolic content of the hydrolysate and organic solvent extract, a calibration curve was constructed ($y=0.0001x+0.0397$, $R^2=0.9950$), and the measurement was expressed as mg phloroglucinol equivalent/g dried sample.

2.9.2. Total flavonoid content (TFC)

To determine the overall flavonoid content of the *E. stolonifera* hydrolysate and organic solvent extract, 75 μL of a solution containing 7.5% sodium nitrite was added to

125 μL of the hydrolysate. After 6 min, a solution consisting of 150 μL of 40% aluminum chloride was added and left for 5 min. Next, 750 μL of a 1M NaOH solution was added, along with distilled water to make the total volume 2.5 mL. After vortexing for 10 sec and incubating for 15 min, the reaction was measured three times at an absorbance of 510 nm using a spectrophotometer from BioTek Instruments in Winooski, Vermont. Quercetin from Sigma Chemical Co. was used as the standard substance and after calibration ($y=0.0031x+0.0534$, $R^2=0.9917$), the total flavonoid content of the hydrolysate and organic solvent extract was expressed as mg quercetin equivalent/g of dried sample.

2.10. Analysis of Sugar content

2.10.1. Total sugar content (TSC)

The total sugar content of the *E. stolonifera* hydrolysate and organic solvent extract was quantified using the methodology outlined by Meillisa A. (2015) (Meillisa et al., 2015). Initially, 0.75 mL of the hydrolysate was mixed with 2.25 mL of concentrated sulfuric acid. Subsequently, 0.45 mL of a 40% phenol solution was added and thoroughly mixed. The reaction was executed through boiling for 5 min and then cooled to room temperature. The spectrophotometer (BioTek Instruments, Winooski, VT, USA) measured the absorbance three times at 490 nm. To determine the total sugar content, glucose from Sigma Chemical Co. (USA) was utilized as the standard material. A cal-

ibration curve (y=0.0033x+0.1191, R^2=0.9994) was then constructed and used to express the sugar content of the hydrolysate and organic solvent extract in mg glucose equivalent/g dried sample.

2.10.2. Reducing sugar content (RSC)

The content of reducing sugar in both the *E. stolonifera* hydrolysate and the organic solvent extract was determined using the 3,5-dinitrosalicylic acid (DNS) colorimetric method, as outlined by Saqib A. A. N. (2015) (Saqib & Whitney, 2015). To prepare the DNS solution, 2 g of dinitrosalicylic acid and 60g of sodium potassium tartrate (Rochele salt) were dissolved in 160 mL of 0.5 N NaOH, with distilled water added to achieve a final volume of 200 mL. Next, 1 mL of the hydrolysate and 4 mL of the DNS solution were combined, and the mixture was boiled in water for 5 min before cooling it to room temperature. Using a spectrophotometer (BioTek Instruments, Winooski, VT, USA), the absorbance was recorded three times at 490 nm. Glucose (Sigma Chemical Co., USA) was utilized as the standard, and after calibration (y=0.0008x+0.1438, R^2=0.9957), the reducing sugar content of the hydrolysate and organic solvent extract was expressed as mg glucose equivalent/g of dried sample.

2.11. Antihypertensive activity

The antihypertensive activity of the hydrolysate from *E. stolonifera* was assessed using the Dojindo ACE Kit-WST, following the instructions and procedures outlined by Wei (2019) (Wei et al., 2019). A 1% solution of the lyophilized powder in water was prepared using HPLC. The enzyme solution was created by dissolving enzyme B in 2 mL of HPLC water and injecting 1.5 mL into enzyme A. Similarly, the indicator solution was formed by dissolving enzyme C and coenzyme in 3 mL of HPLC water each, followed by injecting 2.8 mL of the combined solution into the indicator.

In a 96-well plate, 20 μL of the sample solution was added to both the sample and the sample blank wells. Distilled water, in an amount of 20 μL, was added to the blank 1, blank 2, and sample blank wells. Moreover, the sample, blank 1, and blank 2 wells were treated with 20 μL of Substrate Buffer, while the blank 2 and sample blank wells received 20 μL of distilled water. Additionally, 20 μL of enzyme working solution was added to the sample and blank 1 wells. The plate was then incubated at 37℃ for 1 hr. Finally, 200 μL of distilled water was added to the blank sample, followed by the addition of 200 μL of the indicator working solution to the sample wells, blank 1, and blank 2. The mixture was allowed to react for 10 min, and the absorbance was measured three times at 450 nm using a spectrophotometer (BioTek Instruments, Winooski, Vermont). The measurements were repeated, with captopril (1%) used as the standard. The antihypertensive activity of the hydrolysate was expressed as a percentage using the following formula, 6.

$$\text{Inhibitory activity (\%)} = \frac{A_{blank\,1} - (A_{sample} - A_{sample\,blank})}{A_{blank\,1} - A_{blank\,2}} \times 100 \cdots\cdots\cdots (6)$$

2.12. Antidiabetic activity

The antidiabetic activity of *E. stolonifera* hydrolysate was assessed with a slight modification of the method outlined by Wang X. (2023) (Wang et al., 2023). First, the lyophilized powder was diluted in water for 200mM potassium phosphate buffer (pH 6.8). Next, both the sample solution and α-glucosidase solution (0.2 unit/mL) were added to a 96-well plate, in quantities of 50 μL each, and allowed to react for 10 min in a 37℃ incubator. Positive controls were subjected to the same conditions. After the reaction, we injected the solution of p-nitrophenyl-α-d-glucopyranoside and allowed it to react for another 10 min inside a 37℃ incubator. We measured the absorbance thrice at 405 nm using a spectrophotometer (BioTek Instruments, Winooski, VT, USA). As a positive control, we established a calibration curve using acarbose (Sigma Chemical Co., USA) (R^2=0.9572). The IC_{50} value was obtained by diluting the α-glucosidase inhibitor to a certain concentration, and the resulting concentration of the inhibitor that inhibits 50% of α-glucosidase activity was reported. The hydrolysate's antidiabetic activity was calculated using the given equation (7).

$$\text{Inhibition activity (\%)} = \frac{A_{control} - (A_{sample} - A_{background})}{A_{control}} \times 100 \cdots\cdots\cdots (7)$$

2.13. Anti-inflammatory activity

The protein denaturation inhibition method, as modified by Chamika, W. A. S. (2021), was slightly adjusted to measure the anti-inflammatory activity of the *E. stolonifera* hydrolysate (Chamika et al., 2021). A 1% solution was prepared by diluting the freeze-dried sample in water for HPLC. Subsequently, 500 μL of the prepared sample solution was mixed with egg white albumin solution (6.6% v/v in PBS, pH 6.4) and incubated for 15 min at 37℃ before reacting at 70℃ for 5 min. The mixture was then cooled to room temperature. Absorbance was measured three times at 660 nm using a spectrophotometer from BioTek Instruments in Winooski, VT. As a positive control, Diclofenac sodium (1%) was utilized, and the anti-inflammatory activity of the hydrolysate was calculated in percentage using the formula provided below (8).

$$\text{Inhibition activity (\%)} = \frac{A_{control} - (A_{sample} - A_{background})}{A_{control}} \times 100 \cdots\cdots\cdots (8)$$

2.14. Statistical analysis

The experimental data were analyzed using SPSS version 27 to determine the mean and standard deviation. Additionally, an analysis of variance and a post-hoc Duncan's multiple comparison test were performed to assess significance between items. A significance test was conducted with a level of significance set at <0.05. Pearson's correlation analysis was employed to assess correlations.

III. Results and discussion

1. Proximate composition analysis

Table 2 presents the general components of dried *E. stolonifera*. The analysis revealed moisture content of 8.18% ± 0.01%, ash content of 41.83% ± 0.12%, protein content of 15.30% ± 0.01%, lipid content of 8.97% ± 0.07%, and carbohydrate content of 25.72% ± 0.01%. Brown algae mostly contain fucoidan, laminaran, cellulose, and alginate as primary carbohydrates (Dawczynski et al., 2007). Given that the ash content exhibited the highest percentage, it is evident that *E. stolonifera* is a rich source of minerals.

Table 2. Proximate composition of *E. stolonifera*

Compositions	Raw material (%)
Moisture	8.18 ± 0.01[d]
Ash	41.83 ± 0.12[a]
Crude Protein	15.30 ± 0.01[d]
Crude Lipid	8.97 ± 0.07[c]
Carbohydrate	25.72 ± 0.01[b]

1) Mean ± SD (n=3).

2) Different letters indicate significant differences as per $p<0.05$ by using Duncan's multiple range test.

2. Yield of subcritical water extraction

Table 3 displays the extraction yield of *E. stolonifera* hydrolysate. The minimum yield was 37.88% ± 0.22% at 120℃, while it rose to 62.88% ± 0.19% at 145℃, 75.88% ± 0.18% at 170℃, and 80.24% ± 0.11% at 195℃. An increase in temperature led to a rise in extraction yield, reaching the highest value of 82.81% ± 0.15% at 220℃. As the temperature increases, the production of hydronium ions is believed to promote greater dissolving power, leading to higher yields (Plaza et al., 2013; Haque et al., 2023). Prior research suggests that dispersion forces between the compound and the substrate, as well as hydrogen and dipole-dipole molecular forces, decrease at high temperatures, which, in turn, lowers the activation energy necessary for desorption (Viganó et al., 2016).

Table 3. Hydrolysis efficiency for *E. stolonifera* extracts

Conditions	Yield (%)
120℃	37.88 ± 0.22[e]
145℃	62.88 ± 0.19[d]
170℃	75.88 ± 0.18[c]
195℃	80.24 ± 0.11[b]
220℃	82.81 ± 0.15[a]

1) Mean ± SD (n=3).

2) Different letters indicate significant differences as per $p<0.05$ by using Duncan's multiple range test.

3. Physical properties of hydrolysates

3.1. pH and color

The pH of the hydrolysate of *E. stolonifera* is presented in Table 4. pH gradually decreased with increasing temperature and reached the minimum value of 4.82 ± 0.02 at 195℃, followed by a slight increase to 5.52 ± 0.01 at 220℃. This result is consistent with the previous report stating that acidic substances are created through Maillard reaction, which occurs when basic amino acids react with sugars during high-temperature hydrolysis (Lee et al., 2015). Furthermore, it is hypothesized that the pH appears decreased due to the decomposition of sugars into organic acids (Sasaki et al., 1998). A study conducted previously has reported that treatment of sucrose with subcritical water resulted in decomposition of glucose and fructose products into acidic compounds, with subsequent pH decrease (Gao et al., 2014).

Table 5 depicts color measurement outcomes of the *E. stolonifera* in relation to temperature. As the temperature increased, the value of brightness L* decreased, while the value of a* (red-green) increased. The highest value of b* (yellow-blue) was observed at 145℃, and it is believed that temperature does not significantly affect this value.

Table 4. pH properties of *E. stolonifera* extracts

Conditions	pH
120℃	6.02 ± 0.01[b]
145℃	5.62 ± 0.05[c]
170℃	4.93 ± 0.01[e]
195℃	4.82 ± 0.02[f]
220℃	5.52 ± 0.01[d]

1) Mean ± SD (n=3).

2) Different letters indicate significant differences as per $p<0.05$ by using Duncan's multiple range test.

Table 5. Color properties of *E. stolonifera* extracts

Conditions	L*	a*	b*
120℃	46.29 ± 0.62[a]	0.75 ± 0.19[d]	12.18 ± 0.41[a]
145℃	45.16 ± 0.67[a]	3.05 ± 0.79[c]	13.62 ± 2.13[a]
170℃	34.81 ± 0.31[c]	7.28 ± 0.17[b]	5.41 ± 0.10[d]
195℃	36.99 ± 0.27[b]	9.79 ± 0.97[a]	9.88 ± 0.81[b]
220℃	36.07 ± 0.64[b]	8.81 ± 0.66[a]	7.86 ± 0.88[b]

1) Mean ± SD (n=3).

2) Different letters indicate significant differences as per $p<0.05$ by using Duncan's multiple range test.

4. High Performance Liquid Chromatography (HPLC) of hydrolysates

Table 6 displays the HPLC temperature analysis of phenol compounds in the hydrolysate. The phenol compound analysis revealed that gallic acid, chlorogenic acid, catechin, 4-hydroxybenzoic acid, vanillin, and naringin are present in *E. stolonifera* hydrolysate. Notably, the hydrolysate contents of gallic acid, catechin, and vanillin were high. Gallic acid is a natural phenolic compound that occurs in fruits, and medicinal plants. In the food industry, it has been found to have antioxidant, antimicrobial, anti-inflammatory, anticancer, and neuroprotective effects. Additionally, it is used as a flavoring agent and preservative (Kahkeshani et al., 2019). Chlorogenic acid is a polyphenolic compound found in certain plant species, including tea, coffee, cocoa, and citrus fruits and is commonly consumed in the form of beverages (Naveed et al., 2018). According to a study, chlorogenic acid extracted from coffee was found to be effective in reducing blood pressure and could be used in antihypertensive treatment (Wan et al., 2013). Catechins are a type of flavonoid found in various foods, such as tea, apples, persimmons and berries (Isemura et al., 2019). A study conducted on green tea demonstrated that catechins have an apoptosis-inducing effect on cancer cells (Singh et al., 2011). Furthermore, a clinical trial administered a beverage containing catechins to patients with type 2 diabetes, which resulted in the restoration of their ability to secrete insulin, effectively treating their diabetes (Ganeshpurkar et al., 2020). 4-hydroxybenzoic acid is an aromatic hydroxy acid that serves as an intermediate in the synthesis of various bioproducts, including food, cosmetics and pharmaceuticals (Wang et al., 2018). Vanillin,

also known as 4-hydroxy-3-methoxybenzaldehyde, is an important anti-microbial molecule. It has been used as a flavoring agent in food and pharmaceutical preparations. However, the use of synthetic vanillin is highly restricted by food safety organizations (Walton et al, 2003). Recent research has led to the production of natural vanillin from plants, ensuring its safety (Banerjee et al., 2019).

Table 6. Phenolic compounds profiles of *E. stolonifera* dried samples (mg (100 g)-1 dried biomass) obtained at different hydrolysis conditions

Conditions	Gallic acid	Chlorogenic acid	Catechin	4-hydroxybenzoic acid	Vanillin	Naringin
120℃	11.85 ± 0.44^{d}	N.D.	N.D.	N.D.	N.D.	11.52 ± 0.02
145℃	128.24 ± 1.84^{c}	N.D.	34.27 ± 3.55^{c}	N.D.	N.D.	25.10 ± 1.22
170℃	186.95 ± 0.80^{a}	12.86 ± 1.22^{c}	67.57 ± 1.54^{b}	28.56 ± 0.58^{b}	86.20 ± 1.33^{b}	N.D.
195℃	187.95 ± 1.97^{a}	41.97 ± 0.55^{a}	69.21 ± 2.71^{b}	35.93 ± 0.14^{a}	124.69 ± 2.63^{a}	N.D.
220℃	158.61 ± 2.71^{b}	27.69 ± 1.16^{b}	73.33 ± 2.82^{a}	29.19 ± 0.52^{b}	34.18 ± 1.12^{c}	N.D.

1) Mean ± SD (n=3).

2) N.D., not detected.

2) Different letters indicate significant differences as per $p<0.05$ by using Duncan's multiple range test.

5. Analysis of antioxidant activity of hydrolysates

The figures in Figure 4 display the outcomes of the $ABTS^{+}$ radical scavenging potency of *E. stolonifera*'s hydrolysate. The antioxidant effectiveness grew as the temperature increased, and the highest activity was observed at 195℃ at 35.98 ± 0.14 mg trolox equivalent/g dried sample activity. Consequently, this suggests that under subcritical conditions, more beneficial substances may be extracted because the dielectric constant lowers and becomes similar to that of the organic solvent. This study exhibits a comparable trend to a prior examination that contrasted seaweed extracts and organic solvent extracts by temperature (Park et al., 2022).

Figure 5 showcases the outcomes of DPPH radical scavenging proficiency of *E. stolonifera* hydrolysate. Similar to the $ABTS^{+}$ radical scavenging ability results, antioxidant activity progressively increased with temperature, and the highest antioxidant activity of 38.18 ± 0.49 mg trolox equivalent/g dried sample was observed at 195℃. The tendency for antioxidant activity to rise with temperature was noted as the dielectric constant of subcritical water decreased at high temperatures, facilitating antioxidant extraction (Haque et al., 2023).

Ferrous ion reducing power (FRAP) measures antioxidant capacity, with Figure 6 displaying the FRAP results for *E. stolonifera* hydrolysate and the organic solvent. Consistent with prior antioxidant activity findings, the highest activity was observed at 25.29±0.31 mg trolox equivalent/g dried sample at 195℃. FRAP evaluates the ability of antioxidant elements to reduce iron oxidizer (Fe^{3+}) to iron complex (Fe^{2+}) through

electronic transfer (O'Sullivan et al., 2011). The antioxidant activity is believed to have been influenced by the redox reaction of phenolic compounds found in seaweed.

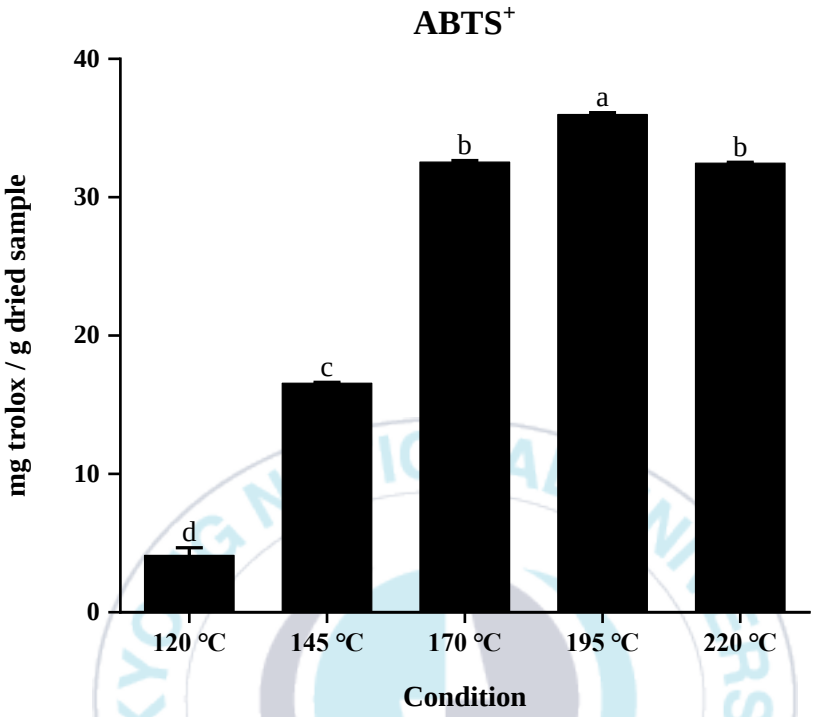

Figure 4. ABTS^{+} radical scavenging properties of *E. stolonifera* hydrolysis obtained by subcritical water hydrolysis

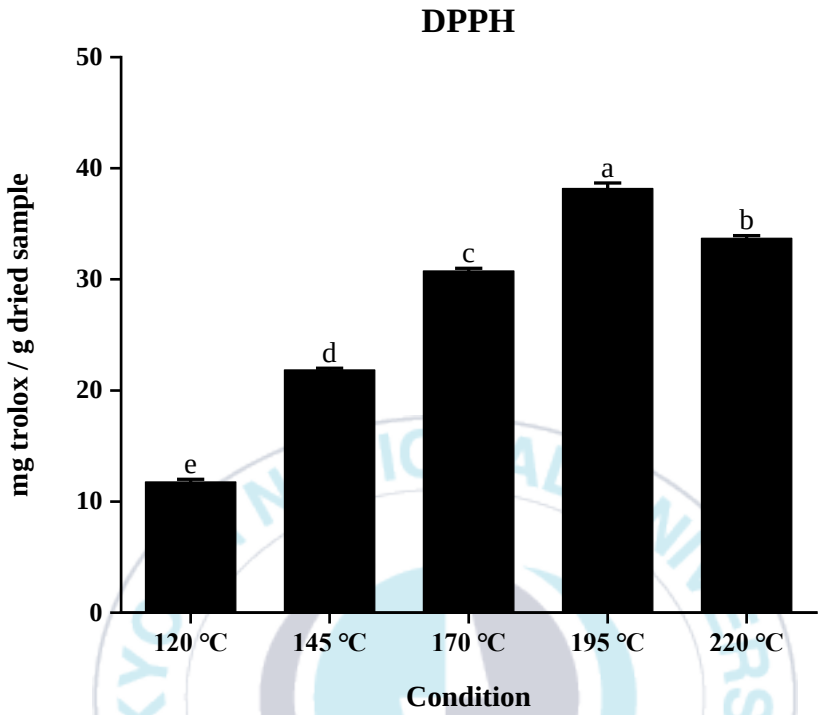

Figure 5. DPPH radical scavenging properties of *E. stolonifera* hydrolysis obtained by subcritical water hydrolysis

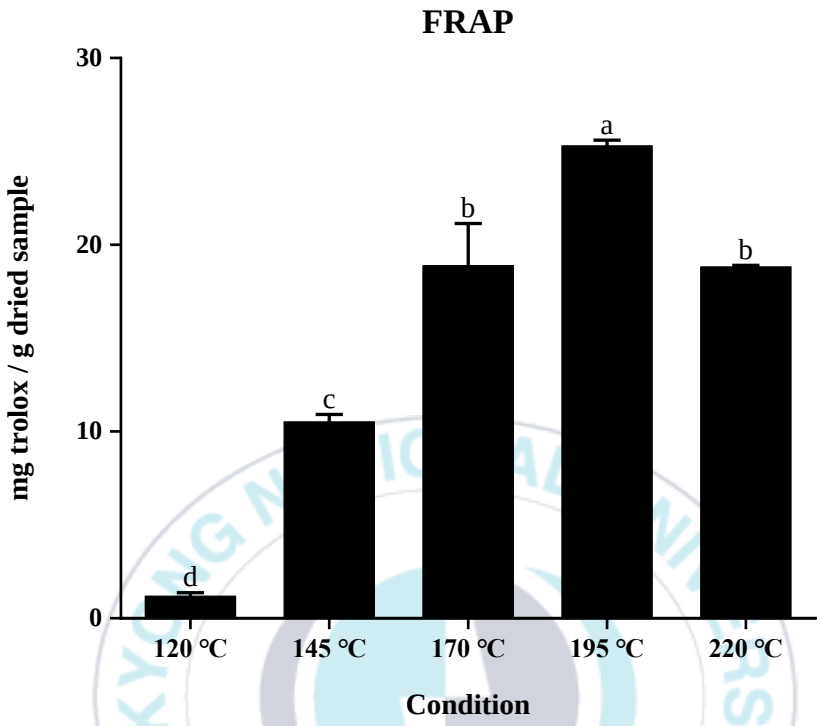

Figure 6. FRAP properties of *E. stolonifera* hydrolysis obtained by subcritical water hydrolysis

6. Analysis of phenol content of hydrolysates

Figure 7 illustrates the results presenting the total phenol content of the hydrolysate of *E. stolonifera*. As the temperature increased, it peaked at 26.02 ± 0.05 mg phloroglucinol equivalent/g dried sample at 195℃ and slightly declined to 23.78 ± 0.15 mg phloroglucinol equivalent/g dried sample at 220℃. Previous studies have demonstrated that phlorotannins, the primary polyphenolic compounds in brown algae, exhibit biological activities, including antiviral, antioxidant, antibacterial, and anticancer properties (Park et al., 2022).

Figure 8 displays the results of the total flavonoid content in *E. stolonifera* hydrolysate. The content of flavonoids increased as the hydrolysis temperature increased, reaching its highest value of 8.40 ± 0.18 mg quercetin equivalent/g dried sample at 195℃. Subsequently, it was observed that the total flavonoid content decreased slightly at higher temperatures. These results demonstrated a comparable pattern to the antioxidant activity, establishing a relationship between flavonoids and antioxidant substances.

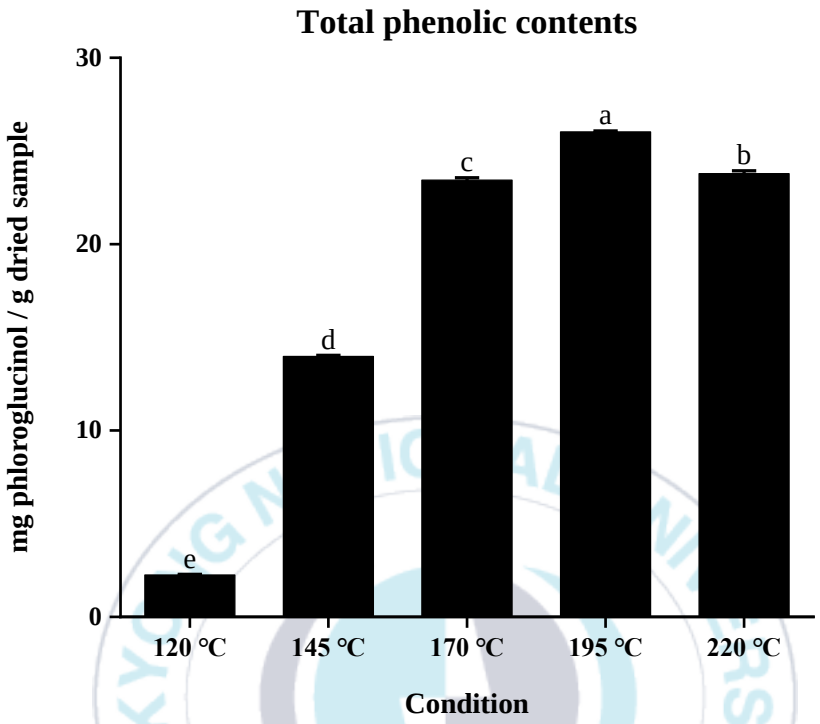

Figure 7. Total phenolic content properties of *E. stolonifera* hydrolysis obtained by subcritical water hydrolysis

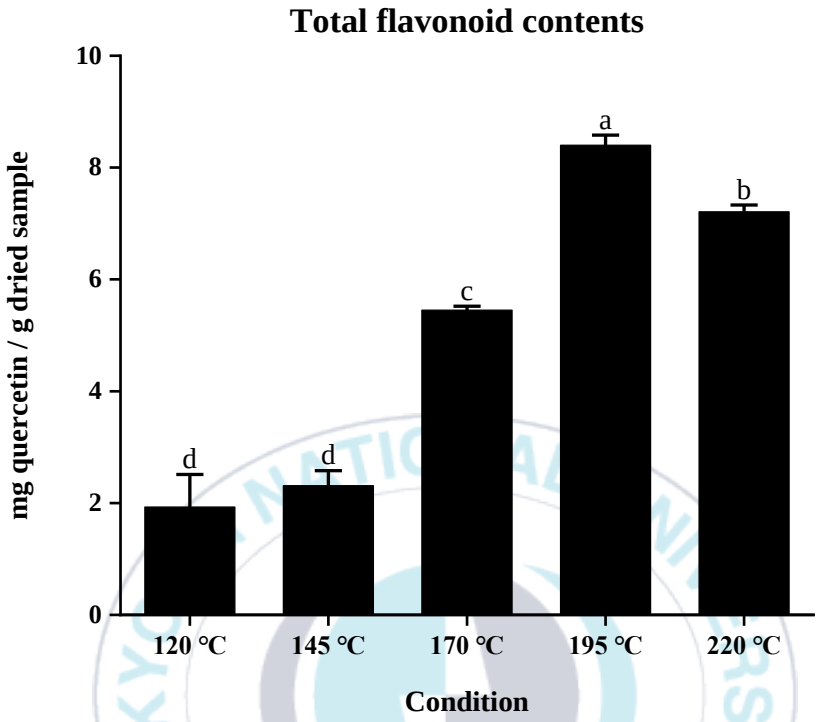

Figure 8. Total flavonoid content properties of *E. stolonifera* hydrolysis obtained by subcritical water hydrolysis

7. Sugar content analysis of hydrolysates

The total sugar content of the hydrolysate of *E. stolonifera* was analyzed using the phenolsulfuric acid method to determine the amount of sugar that could be converted into bioenergy. Figure 9 indicates that at 120℃, the total sugar content was at its highest, measuring 102.04 ± 1.07 mg glucose equivalent/g dried sample and showed a decreasing trend with rising temperature. At 220℃, the sugar content was 24.15 ± 1.08 mg glucose equivalent/g dried sample, indicating a slight increase. It has been confirmed that the decrease in total sugar content as temperature increases is related to reports indicating that total sugar content can be reduced due to caramelization and browning reactions (Moon et al., 2005). The total sugar content results exhibited similar trends to vermicompost subcritical water extracts previously studied (Park et al., 2022).

Figure 10 shows the reducing sugar content of the hydrolysate of *E. stolonifera*. Reducing sugar pertains to sugar that contains an aldehyde group, which gets oxidized to a carboxylic acid. It was observed that the hydrolysate of *E. stolonifera* had high reducing sugar content at high temperatures, reaching its peak at 61.83 ± 1.63 mg glucose equivalent/g dried sample at 195℃. Further research is still needed to explore the significant impact of reducing sugars on temperature.

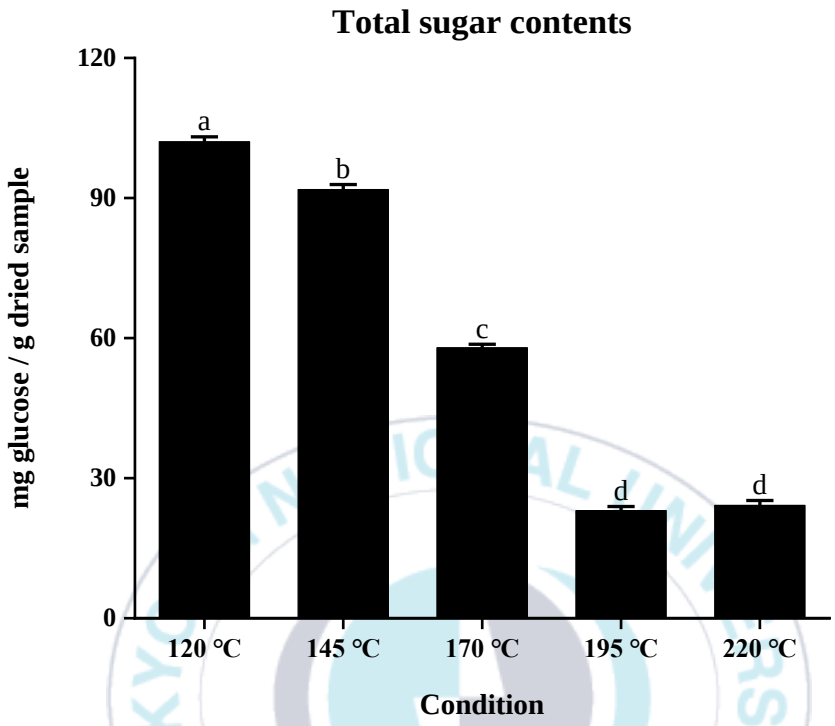

Figure 9. Total sugar content properties of *E. stolonifera* hydrolysis obtained by subcritical water hydrolysis

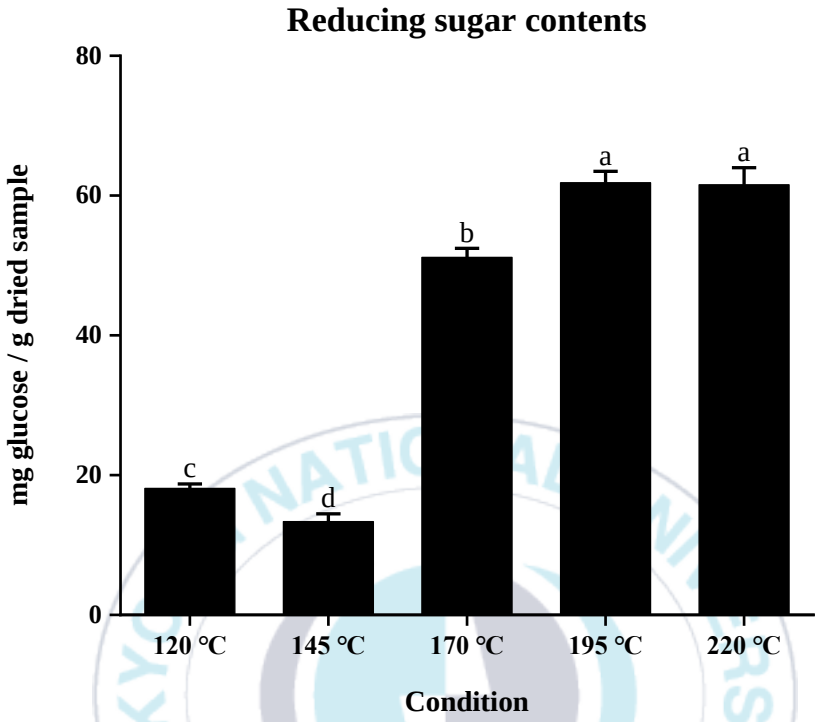

Figure 10. Reducing sugar content properties of *E. stolonifera* hydrolysis obtained by subcritical water hydrolysis

8. Analysis of optimum extraction conditions using response surface methodology (RSM)

8.1. Optimization of extraction conditions

The aim of this investigation was to identify extraction conditions that improve the overall phenol content. The anticipated and observed data for the experimental conditions formulated by response surface analysis are presented in Table 7. Technical term abbreviations introduced in the text will be explained. It was discovered that the maximum predicted value for total phenol content was 54.58 mg phloroglucinol/g of dehydrated sample after extraction with a rate of 20 (g/mL) at a temperature of 160℃ for 60 min, while the empirical result was 30 (g/mL) at 160℃ for 40 min. When extracted with a liquid-to-solid ratio of mL, the sample yielded the highest value of 53.93 mg phloroglucinol equivalent/g dried sample. A quadratic equation was formulated through statistical analysis of the data, expressing the relationship between total phenol content (Y) and extraction temperature (X_1), extraction time (X_2), and solid-to-liquid ratio (X_3) during extraction (9).

$$Y = 48.14 + 2.03X_1 + 0.36X_2 + 7.85X_3 - 2.90X_1X_2 + 2.56X_1X_3 + 0.13X_2X_3 - 4.63X_1^2 - 1.41X_2^2 - 1.37X_3^2 \cdots\cdots\cdots\cdots\cdots\cdots (9)$$

The regression analysis and analysis of variance results for the quadratic equation are displayed in Table 8. The R^2 value, which indicates the goodness of fit of the response model, was 0.9422, and the p-value was significant at 0.0015. This determination suggests that the quadratic equation is appropriate for predicting response values. With an increase in the solid-to-liquid ratio, there is a tendency for the total phenol content to rise. The three-dimensional response surface graph and contour plot depicting the total phenol content can be seen in Figure 11. Table 9 presents the results of the optimum extraction conditions achieved through response surface analysis. On the other hand, Table 10 showcases the total phenol content predicted under the optimum extraction conditions and the actual experimental values.

Table 7. Box–Behnken design and results of three variables with their observed responses

Run	Temperature (℃)	Time (min)	Ratio (g/mL)	TPC (mg PE/g dried sample)	
				Predicted	Actual
1	230	40	10	53.70	53.08
2	160	40	10	48.14	45.36
3	195	40	20	48.14	48.13
4	195	20	10	48.14	52.60
5	230	20	20	33.76	33.16
6	160	20	20	48.14	47.63
7	160	40	30	52.72	53.93
8	195	40	20	46.67	46.65
9	195	40	20	36.81	35.02
10	230	60	20	34.82	36.01
11	195	60	30	43.33	43.36
12	230	40	30	48.14	47.00
13	195	20	30	45.40	46.03
14	160	60	20	54.58	53.40
15	195	40	20	37.74	36.54
16	195	40	20	41.59	43.42
17	195	60	10	37.28	37.93

1) PE, phloroglucinol equivalent.

Table 8. ANOVA table for *E. stolonifera* total phenolic content

Source	Sum of Squares	df	Mean Square	F Value	P-value Prob>F	
Model	700.32	9	77.81	12.67	0.0015	significant
X_1-Temperature	32.84	1	32.84	5.35	0.0540	
X_2-Time	1.03	1	1.03	0.17	0.6949	
X_3-Ratio	492.88	1	492.88	80.26	< 0.0001	
X_1X_2	33.53	1	33.53	5.46	0.0521	
X_1X_3	26.11	1	26.11	4.25	0.0781	
X_2X_3	0.071	1	0.071	0.012	0.9175	
X_1^2	90.09	1	90.09	14.67	0.0065	
X_2^2	8.31	1	8.31	1.35	0.2827	
X_3^2	7.89	1	7.89	1.28	0.2943	
Residual	42.98	7	6.14			
Lack of Fit	13.82	3	4.61	0.63	0.6321	not significant
Pure Error	29.16	4	7.29			
Cor Total	743.30	16				

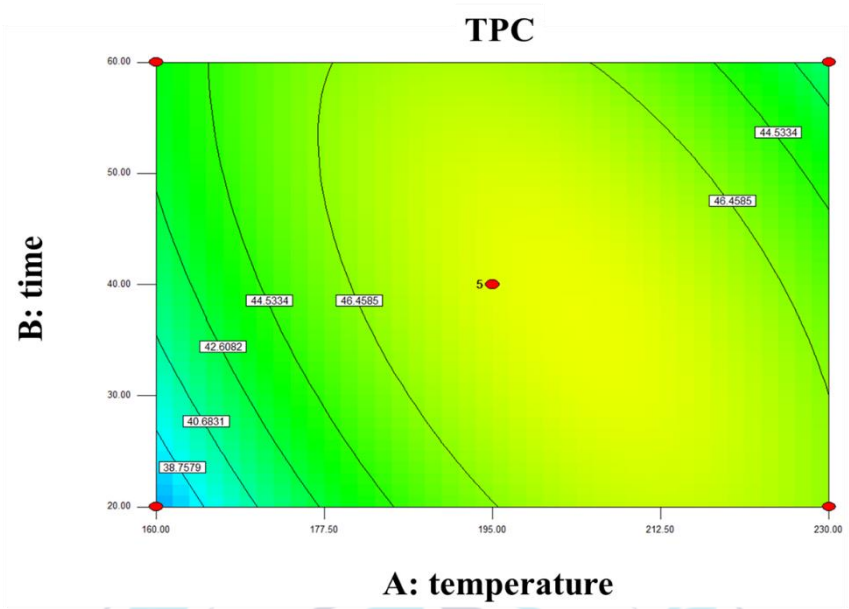
TPC
B: time
A: temperature
60.00
50.00
40.00
30.00
20.00
160.00
177.50
195.00
212.50
230.00
44.5334
46.4585
42.6082
40.6831
38.7579
5

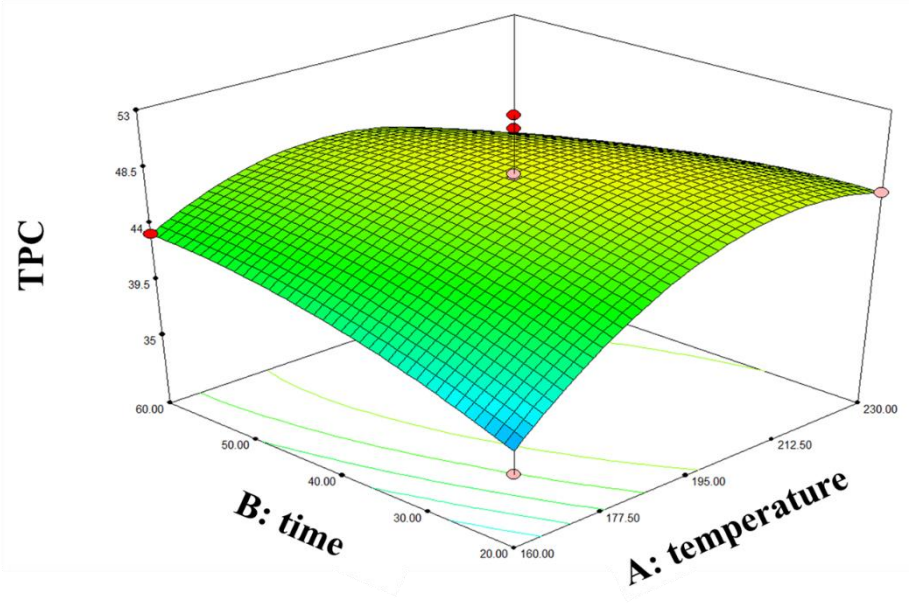
TPC
53
48.5
44
39.5
35
B: time
60.00
50.00
40.00
30.00
20.00
A: temperature
160.00
177.50
195.00
212.50
230.00

(a)

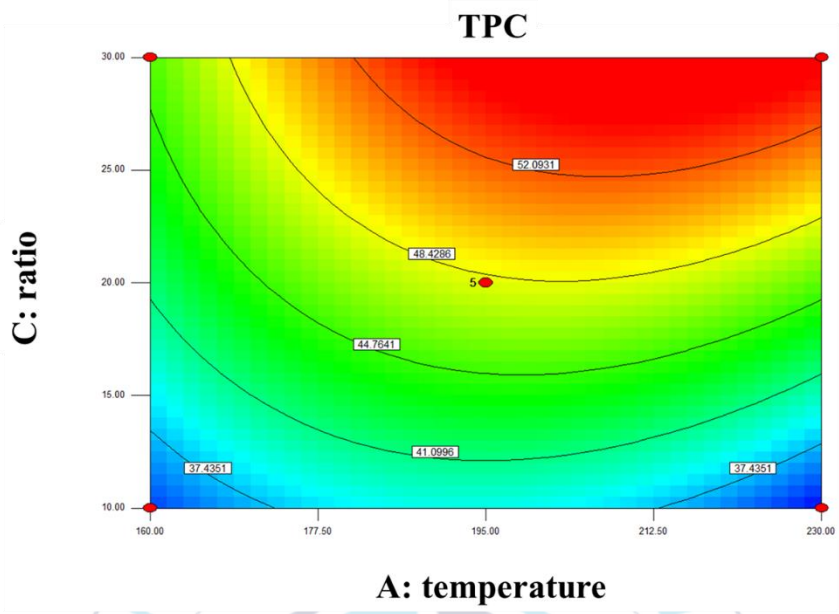
TPC
C: ratio
A: temperature
30.00
25.00
20.00
15.00
10.00
160.00
177.50
195.00
212.50
230.00
52.0931
48.4286
5
44.7841
41.0996
37.4351
37.4351

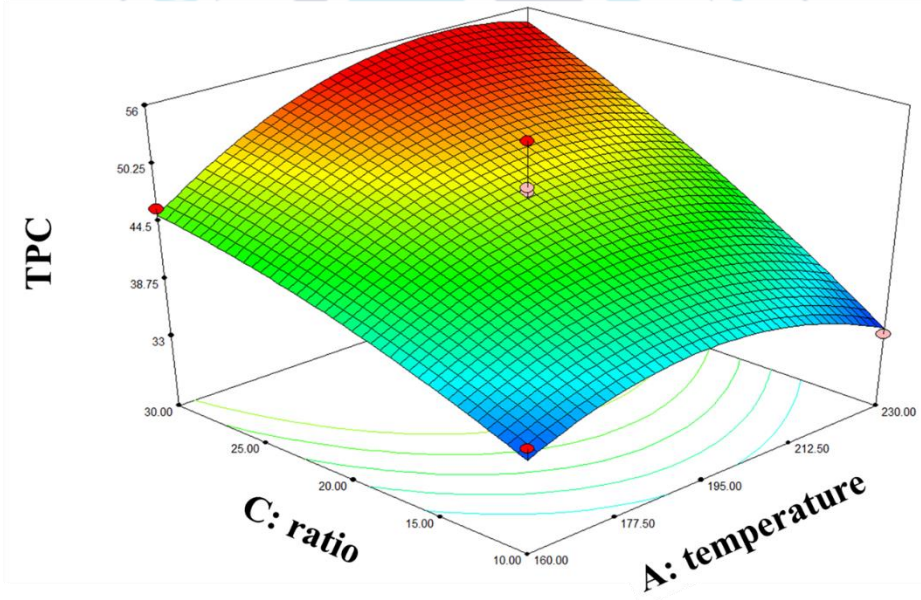
TPC
56
50.25
44.5
38.75
33
30.00
25.00
20.00
15.00
10.00
C: ratio
160.00
177.50
195.00
212.50
230.00
A: temperature

(b)

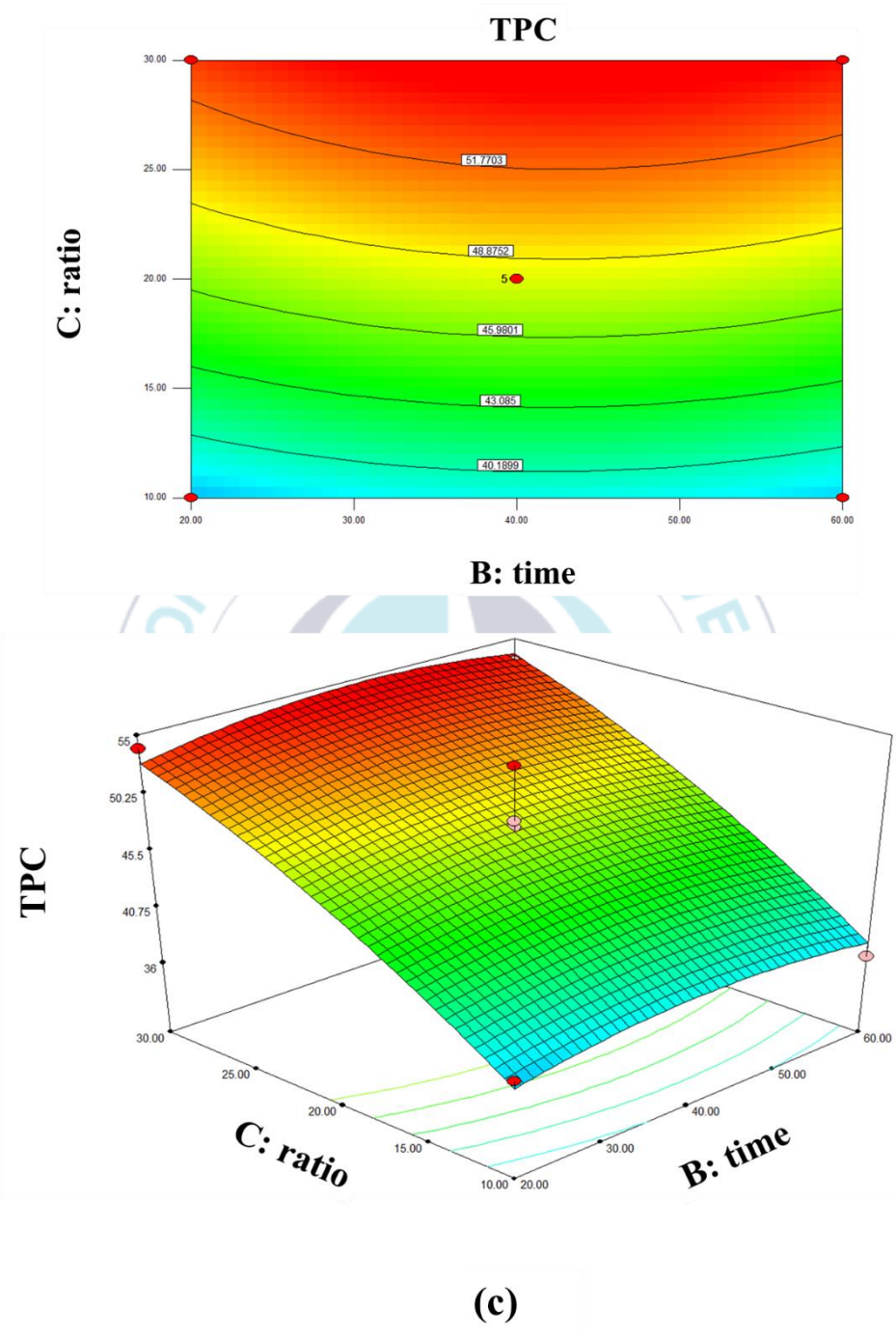

Figure 11. The contour plots and three-dimensional plots of TPC

(a) temperature and time; (b) temperature and ratio; (c) time and ratio

Table 9. Predicted optimum extraction conditions of OCE-ES

	Temperature (℃)	Time (min)	Ratio (g/mL)
Optimum condition	198.50	36.21	12.23

Table 10. Comparison of predicted and actual values of the responses at optimum extraction conditions

	Predicted value	Actual value
TPC (mg PE/g)	54.69	50.01 ± 0.12

1) Mean ± SD (n=3).

2) PE, phloroglucinol equivalent.

8.2. Maillard reaction products (MRPs) of optimized extract

The Maillard reaction is a chemical process that exemplifies non-enzymatic browning reactions. Heat generates amino groups of proteins and carbonyl groups of sugars in this reaction (Saravana et al., 2016). The melanoidin, which is the end product of the Maillard reaction, acts as a brown pigment in cooked foods and significantly affects food quality characteristics such as taste, aroma, color, and texture (Gereniu et al., 2017). The MRPs of the extract were measured at an absorbance of 294 nm and 420 nm, expressed as 11.35 ± 0.12 absorbance units (A.U.). Measuring MRPs by absorbance at specified wavelengths is a valuable approach to assess the degree of the Maillard reaction in processed foods. This allows for the optimization of processing conditions and the management of product quality.

Table 11. MRPs properties of OCE-ES and EE

	MRPs		
	294 nm	**420 nm**	**294/420**
OCE-ES	3.704 ± 0.007	0.326 ± 0.003	11.353 ± 0.117
EE	1.933 ± 0.010	2.371 ± 0.018	0.815 ± 0.005

1) Mean ± SD (n=3).

8.3. Heavy metal contents

Heavy metals are typically found in low concentrations in aquatic ecosystems. However, due to industrial and water pollution, their concentration has increased, leading to environmental issues. In humans, heavy metals can cause fatal diseases such as nervous system damage, reproductive disorders, and cancer (Haidar et al., 2023). Table 12 displays the results of heavy metal presence in OCE-ES and raw powder. The raw powder was found to contain 0.102 μg/kg of As, 0.001 μg/kg of Cd, and 0.003 μg/kg of Pb, while OCE-ES had 0.062 μg/kg of As and 0.001 μg/kg of Cd. Both the raw powder and OCE-ES were found to have acceptable levels of heavy metals. Notably, subcritical water extraction led to a decrease in Pb and As.

Table 12. Presence of heavy metals in OCE-ES and raw powder

	Heavy metal (μg/kg)		
	As	**Cd**	**Pb**
Raw powder	0.10206	0.00007	0.00363
OCE-ES	0.06245	0.00016	N. D.
Control	0.00124	N. D.	N. D.

1) Mean ± SD (n=3).

2) N.D., not detected.

8.4. Physical properties of optimized extract

8.4.1. Yield

Table 13 shows the yields of the extract obtained under optimum extraction conditions and the yields from the ethanol extract. The yield of the extract obtained under optimum extraction conditions was 74.51% ± 0.35%, which was significantly higher than the yield of the ethanol extract (14.71% ± 0.13%). This suggests that an increase in temperature can enhance surface contact for active mass transfer to the solvent, allowing the solvent to penetrate the sample's structure (Plaza et al., 2013). The yield of ethanol extraction was lower than that of subcritical water extraction, despite ethanol's low dielectric constant as a solvent. This demonstrates that subcritical water extraction is a safer method compared to organic solvents, which typically have higher yields but greater risks. Therefore, it is suitable for extraction in food applications.

Table 13. Yield properties of OCE-ES and EE

	Yield (%)
OCE-ES	74.51 ± 0.35
EE	14.71 ± 0.13

1) Mean ± SD (n=3).

8.4.2. pH and color

Table 14 presents the pH values of the extracts under optimum conditions and ethanol. The extract under optimum conditions had a pH of 4.75 ± 0.02, while the ethanol extract had a pH of 6.18 ± 0.01, which is relatively neutral compared to the extract under optimum conditions. Previous studies have reported that reducing sugars produced by the browning reaction at high temperatures can decompose into organic acids, which lower the pH (Getachew et al., 2017).

Table 15 presents the chromaticity results of the extract and ethanol extract under the optimum extraction conditions. The L*, a*, and b* values of the extract under these conditions were 33.67 ± 0.10, 5.19 ± 0.01, and 3.65 ± 0.02, respectively. The corresponding values for the ethanol extract were 40.56 ± 0.35, -8.47 ± 0.40, and 11.82 ± 0.77, respectively. Color is a crucial factor that affects product crystallinity in the food industry. Compared to the ethanol extract, the extract obtained under optimum extraction conditions in this experiment showed a decrease in the L* and b* values, while the a* value tended to increase. This change could be attributed to the extraction of pigments based on carotenoids or the conversion and browning reaction of macromolecules.

Table 14. pH properties of OCE-ES and EE

	pH
OCE-ES	4.75 ± 0.02
EE	6.18 ± 0.01

1) Mean ± SD (n=3).

Table 15. Color properties of OCE-ES and EE

	Color		
	L*	**a***	**b***
OCE-ES	33.67 ± 0.10	5.19 ± 0.01	3.65 ± 0.02
EE	40.56 ± 0.35	-8.47 ± 0.40	11.82 ± 0.77

1) Mean ± SD (n=3).

8.5. Analysis of FT-IR of optimized extract

Figure 12 shows the FT-IR results for the lyophilized powder of the optimized hydrolysate and ethanol extract. FT-IR is a technique that measures the degree of energy absorption of an analytical sample as a function of wavelength, providing information about the substances present in the sample. The raw powder, optimal and ethanolic extract powder all exhibit five identical wavelengths. These include the O-H group at wavelengths from 3200 to 3550 cm^{-1}, C-H group at wavelengths from 2840 to 3000 cm^{-1}, -C≡C- group at wavelengths from 2100 to 2240 cm^{-1}, O-C-O group at wavelengths from 1530 to 1630 cm^{-1}, and finally C-O group at wavelengths from 1000 to 1150 cm^{-1} (Rajeswari et al., 2019; Leal et al., 2008). Additionally, the raw powder exhibited wavelengths corresponding to the C-O-S group, the optimized extract exhibited wavelengths corresponding to the C-N group and the ethanol extract exhibited wavelengths corresponding to the C=O group (Ho et al., 2023). The peak of the wavelength in the optimized extract was larger, indicating a significant change in the molecule's structure during the subcritical water extraction process.

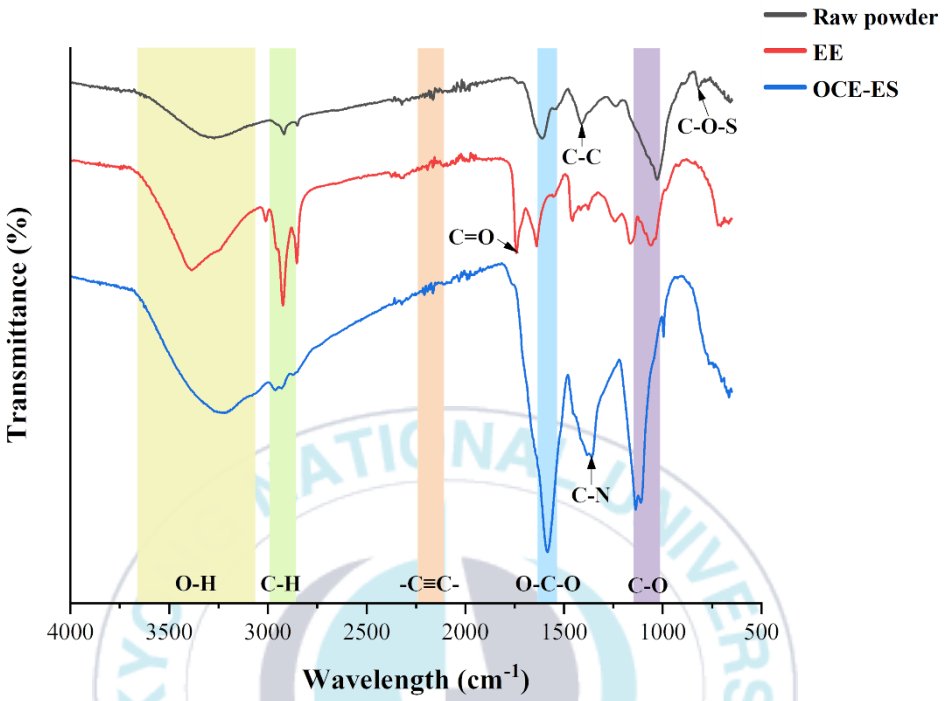

Figure 12. FT-IR spectrum of raw powder, EE and OCE-ES

8.6. Analysis of XRD of optimized extract

Figure 13 shows the XRD results of the freeze-dried optimized hydrolysate sample. XRD is a technique that uses X-rays to reveal the molecular structure and represent their arrangement (Khan et al., 2020). Seaweed typically contains alkali metals such as K and Na. When extracting algae at high temperatures, alkali metals are converted to a gaseous state under high vapor pressure. X-ray diffractometer analysis revealed that the alkali metal elements K and Na can exist in both oxide and chloride forms. Peaks were observed at 42.00˚, 40.56˚, 50.24˚, and 66.40˚ for KCl and at 2θ=27.44˚, 31.80˚, 45.50˚, 56.54˚, 66.28˚, and 75.34˚ for NaCl. The raw powder, freeze-dried sample of the optimized hydrolysate, and freeze-dried sample of the ethanol extract were found to contain KCl (Wang et al., 2008; Nunes et al., 2017; Cao et al., 2021). However, the raw powder contained predominantly KCl, while the lyophilized powder of the optimized hydrolysate and ethanol extract had a high content of NaCl. Previous studies have shown that kelp, a type of brown algae, has a high concentration of K followed by Na. The raw kelp powder was found to have a high concentration of KCl, while NaCl was found to be high after temperature treatment. The high KCl content in the raw powder is due to the fact that Na is less reactive than K. This is because K has a high ionization potential and relatively low ionization energy (Boakye et al., 2018).

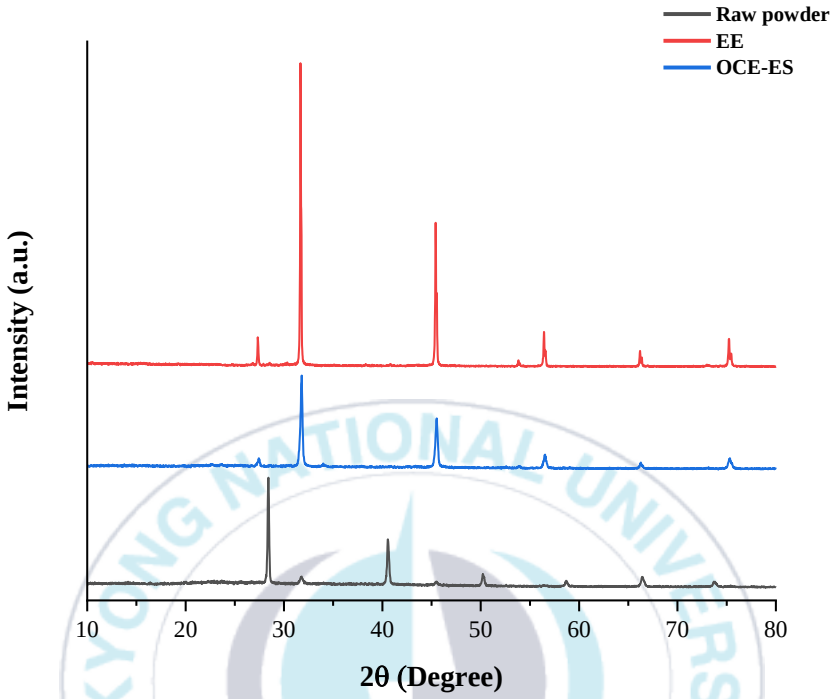

Figure 13. XRD curves of raw powder, EE and OCE-ES

8.7. Analysis of HPLC of optimized extract

Table 16 displays the analysis of phenolic compounds from the extract conducted under optimum extraction conditions. The presence of five commonly found types of phenols in seaweed was examined. Among them, 4-hydroxybenzoic acid exhibited the highest content at 1674.89 ± 0.08 μg/g. Chlorogenic acid measured 704.88 ± 1.09 μg/g, rutin was observed at 674.95 ± 0.15 μg/g, gallic acid at 135.64 ± 0.07 μg/g, and 4-hydroxy-3,5-dimethoxycinnamic acid measured 114.06 ± 0.09 μg/g (Figure 14). Compared to the previous analysis of temperature-specific extracts for phenolic compounds, two additional compounds were identified: rutin and 4-hydroxy-3,5-dimethoxycinnamic acid. Rutin is a flavonoid glycoside of quercetin and rutinose, commonly found in plant-derived foods such as fruits, vegetables, and wine. Previous studies have reported that rutin modulates molecular networks of signal transduction in several cancer cells (Imani et al., 2021). 4-hydroxy-3,5-dimethoxycinnamic acid is a hydroxycinnamic acid commonly found in plants. It has antioxidant properties and has been reported to exhibit antimicrobial effects. This compound has potential applications in the food, cosmetic, and pharmaceutical industries (Nićiforović et al., 2014). Additionally, *E. stolonifera* contains eckol, dieckol, and triphlorethol-A. Dieckol promotes apoptosis in Hep3B cells, leading to the death of liver cancer cells (Cotas et al., 2020; Yoon et al., 2013).

Table 16. Phenolic compounds profiles of OCE-ES

	Gallic acid	Rutin	4-hydroxybenzoic acid	Chlorogenic acid	4-hydroxy-3,5-dimethoxycinnamic acid
OCE-ES (μg/g)	135.64 ± 0.07	674.95 ± 0.15	1674.89 ± 0.08	704.88 ± 1.09	114.06 ± 0.09
EE	N.D.	N.D.	N.D.	N.D.	N.D.

1) Mean ± SD (n=3).
2) N.D., not detected.

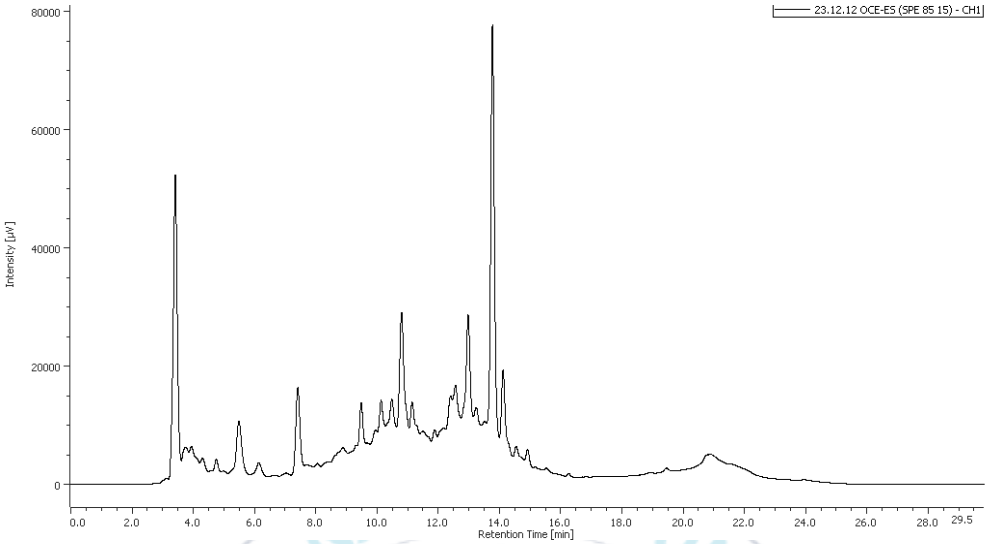

Figure 14. Chromatograms of OCE-ES

8.8. Analysis of antioxidant activity of optimized extracts

Table 17 shows the antioxidant activities of the extract under optimum extraction conditions and the ethanol extract. The $ABTS^{+}$ results of the extract under optimum extraction conditions were 70.94 ± 0.15 mg trolox equivalent/g dried sample, while the ethanol extract showed 0.77 ± 0.11 mg trolox equivalent/g dried sample. The DPPH results were 60.03 ± 0.35 mg trolox equivalent/g dried sample for the former and 22.43 ± 0.24 mg trolox equivalent/g dried sample for the latter. Under optimum extraction conditions, the dried sample displayed an iron ion reducing power of 29.45 ± 0.39 mg trolox equivalent/g, while the ethanol extract showed no activity. Previous research by Pinteus S. (2017) has shown that seaweed extracts have substantial antioxidant capacity due to their radical removal properties (Pinteus et al., 2017). The DPPH analysis technique, an electron transferbased antioxidant analysis method, produces a violet solution in ethanol. Antioxidant molecules are known to reduce free radicals, resulting in an ethanol solution that is colorless (Garcia et al., 2012). The FRAP assay is based on the principle of pH-mediated reduction of Fe^{3+} to Fe^{2+}. As previously reported, reactions at low pH have an iron solubility-preserving effect, reducing ionization potential and increasing redox potential, ultimately leading to hydrogen atom transfer (Cerretani et al., 2010). Subcritical water extraction is believed to have a dielectric constant similar to that of organic solvents, which gives it great dissolving power. This facilitates the extraction of antioxidant substances.

Table 17. Antioxidant activities of OCE-ES and EE

	$ABTS^+$ (mg TE/g)	**DPPH (mg TE/g)**	**FRAP (mg TE/g)**
OCE-ES	70.94 ± 0.15	60.03 ± 0.35	29.45 ± 0.39
EE	0.77 ± 0.11	22.43 ± 0.24	N.D.

1) Mean ± SD (n=3).

2) TE, trolox equivalent; N.D., not detected.

8.9. Analysis of phenol content of optimized extracts

Table 18 shows the total phenol and flavonoid contents of the extract under optimum extraction conditions and the ethanol extract. The extract under optimum extraction conditions exhibited a total phenol content of 50.01 ± 0.12 mg phloroglucinol equivalent/g dried sample, while the ethanol extract demonstrated a total phenol content of 15.42 ± 0.19 mg phloroglucinol equivalent/g dried sample. The results for total flavonoid content were 43.58 ± 0.01 mg quercetin equivalent/g of dried sample and 12.54 ± 0.37 mg quercetin equivalent/g of dried sample, respectively. Seaweeds are rich in phenolic compounds, which have been found to be highly active. *E. stolonifera* contains representative phenolic compounds such as phloroglucinol, eckstolonol, and dieckol (Kang et al., 2003). Han noted that these compounds possess significant activity (Han et al., 2021). Under optimum extraction conditions, the flavonoid content is believed to be high due to the stabilization of reactive oxygen species by reacting with reactive radical compounds (Farasat et al, 2014).

Table 18. Total phenolic and total flavonoid content profiles of OCE-ES and EE

	TPC (mg PE/g)	TFC (mg QE/g)
OCE-ES	50.01 ± 0.12	43.58 ± 0.01
EE	15.42 ± 0.19	12.54 ± 0.37

1) Mean ± SD (n=3).

2) PE, phloroglucinol equivalent; QE, quercetin equivalent.

8.10. Correlation analysis between antioxidant activity and phenol content

Table 19 shows the correlation analysis between phenolic content and antioxidant activity of the optimal *E. stolonifera* extracts. The results show a significant correlation (R^2=0.997) between the DPPH radical scavenging capacity and ferric ion reducing capacity, as well as a correlation of R^2=0.901 between $ABTS^+$ and total flavonoid content. Previous studies have also reported correlations between the overall phenolic content, total flavonoids, and antioxidant activity (Liu et al., 2011; Farasat et al., 2014). These studies have shown that the high antioxidant activity of extracts is proportional to their high total phenolic and flavonoid content. It is important to note that these findings are based on objective evaluations and are supported by scientific evidence. The higher content of flavonoids and phenolics in the extract has been attributed to this effect. Flavonoids can precipitate the tyrosinase enzyme and act as substrates and inhibitors for tyrosinase, which explains their role in this process (Ali et al., 2021). The study conducted by Liu, C. C. (2011) suggests that phenolic compounds and flavonoids are the main factors and active compounds, respectively, in antioxidant activity (Liu et al., 2011).

Table 19. Pearson's correlation coefficients between chemical properties and biological activities

	ABTS^{+}	DPPH	FRAP	TPC	TFC
ABTS^{+}	1				
DPPH	-0.194	1			
FRAP	-0.200	0.997**	1		
TPC	0.486	0.400	0.338	1	
TFC	0.901*	-0.506	-0.488	0.073	1

1) * The correlation is significant at the 0.05 level, ** The correlation is significant at the 0.01 level.

8.11. Analysis of sugar content of optimized extracts

Table 20 presents the results of a sugar content analysis of the extract under optimum extraction conditions. The potential bioenergy-producing sugars were determined using the phenolsulfuric acid approach. The total sugar content of the extract under optimum extraction conditions and the ethanol extract were 55.06 ± 1.51 mg glucose equivalent/g of dried sample and 1.98 ± 0.17 mg glucose equivalent/g of dried sample, respectively.

Additionally, under the optimal extraction conditions, the amount of reducing sugar was 19.22 ± 0.23 mg glucose equivalent/g of dried sample. This result is consistent with previous findings that suggest caramelization and browning reactions can decrease the total sugar content (Moon et al., 2005). Moreover, elevated temperatures may cause the breakdown of polysaccharides, such as fucoidan, resulting in a reduction of sugar content (Park et al., 2023a). Similarly, previous studies on ginseng and brown algae have also shown that high temperatures lead to a decrease in sugar content (Moon et al., 2005; Park et al., 2022).

Table 20. Total sugar and reducing sugar content profiles of OCE-ES and EE

	TSC (mg GE/g)	RSC (mg GE/g)
OCE-ES	55.06 ± 1.51	19.22 ± 0.23
EE	1.98 ± 0.17	N.D.

1) Mean ± SD (n=3).

2) N.D., not detected.

3) GE, glucose equivalent.

8.12. Analysis of antihypertensive activity of optimized extracts

The effectiveness of the extract as an antihypertensive was established through Angiotensin Converting Enzyme (ACE) inhibition under optimal extraction conditions. The outcomes are depicted in Figure 15. ACE inhibitors treat hypertension by relaxing blood vessels and blocking the conversion of angiotensin I to angiotensin II. Admassu (2018) conducted a recent study that identified a peptide with ACE inhibitory activity isolated from protein hydrolysate. Several studies have investigated the antihypertensive efficacy of seaweed (Admassu et al., 2018; Seca & Pinto, 2018; Ren et al., 1994; Kim et al., 2023). The positive control group utilized Captopril (1%), a well-known therapy for hypertension, which exhibited a potency of ≤99.22% ± 0.01%. The extract, when administered under optimum extraction conditions, showed a considerable activity of ≤95.87% ± 0.01% at a concentration of just 0.5%. According to previous research, the use of natural sources, such as seaweed, for antihypertensive activity is expected to be high due to the lower incidence of side effects compared to synthetic inhibitors (Park et al., 2023a).

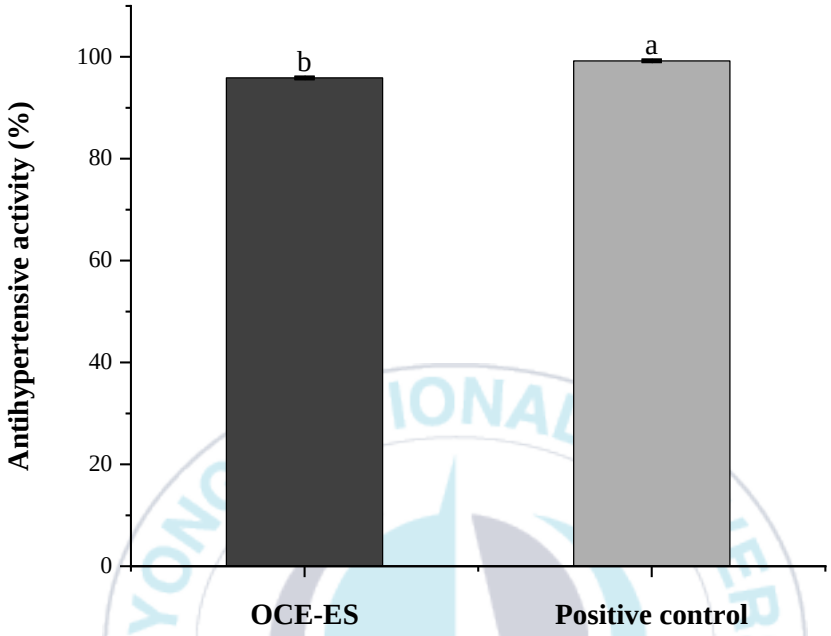

Figure 15. Antihypertensive activity of OCE-ES

8.13. Analysis of antidiabetic activity of optimized extracts

Figure 16 shows the results of the anti-diabetic screening of the optimal extract conditions from *E. stolonifera*. The inhibition of α-glucosidase, which is commonly used as an antidiabetic assay, reduces carbohydrate digestion and thus lowers blood glucose levels (Dowarah et al., 2020). Previous studies have demonstrated the potent antidiabetic activities of flavonoid compounds, particularly tannins (Ghani et al., 2015). In the current experiment, acarbose (1%) was used as a positive control and demonstrated ≤96.68% ± 0.07% activity. The optimized conditioned extract (1%) exhibited ≤69.29% ± 1.83% activity, whereas the ethanol extract showed ≤92.67% ± 1.13% activity. These results are consistent with a previous study that used ethanol extraction on 15 seaweed species (Lordan et al., 2013).

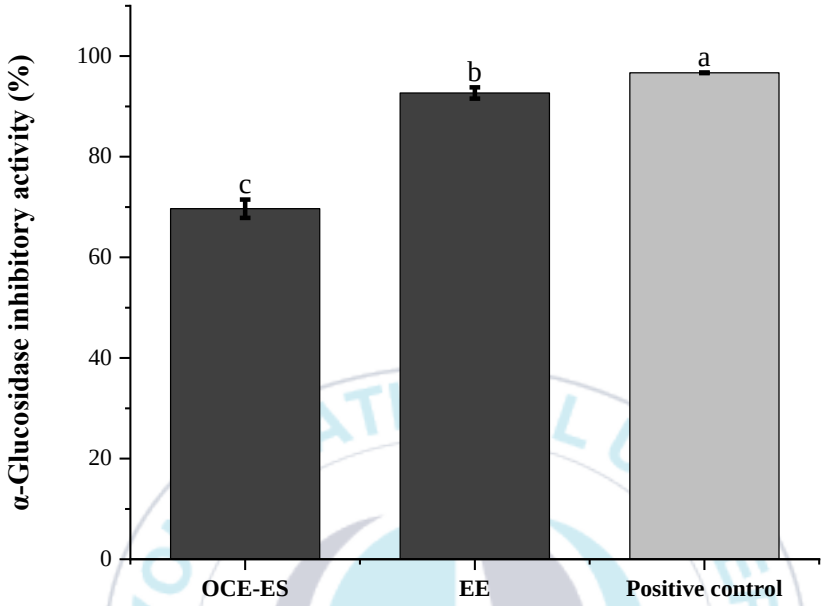

Figure 16. α-Glucosidase inhibitory activity of OCE-ES and EE

8.14. Analysis of anti-inflammatory activity of optimized extracts

Inflammation can cause pain and lead to protein denaturation and membrane deformation (Leelaprakash et al., 2011). Previous research has confirmed that the extract contains flavonoids, flavonones, tannins, and phenolic acids with anti-inflammatory properties (Owoyele et al., 2005). The anti-inflammatory activity of the extract was demonstrated through a protein denaturation inhibition method using optimal extraction conditions. Figure 17 displays the outcomes of an experiment that supports the anti-inflammatory effect. The experiment used diclofenac sodium (1%) as a positive control, which displayed a ≤75.33% ± 0.84% inhibition of protein denaturation. The extract under the optimum extraction conditions demonstrated an inhibitory activity of ≤68.55% ± 0.98%. This was followed by the ethanol extract, which had an inhibitory activity of ≤41.62% ± 0.66%.

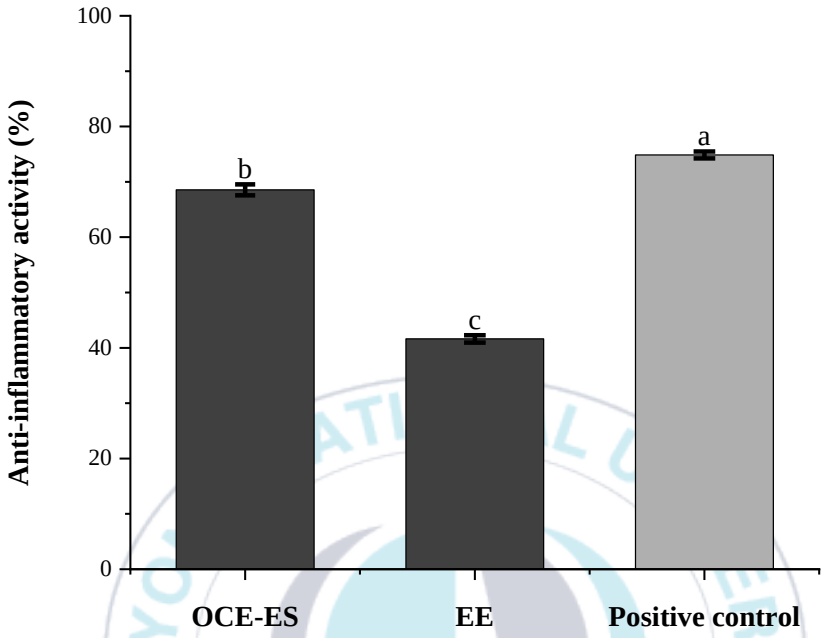

Figure 17. Anti-inflammatory activity of OCE-ES and EE

IV. Conclusions

In this investigation, subcritical water extraction was employed to obtain the hydrolysate of *E. stolonifera*, utilizing an environmentally friendly extraction method. The *E. stolonifera* hydrolysate was subsequently subjected to physicochemical analysis and physiological activity assessment through response surface analysis. Optimization variables for the subcritical water extraction process included the reaction temperature, reaction time, and solid-to-liquid ratio.

1) In the response surface analysis, the solid-to-liquid ratio was identified as the most significant factor affecting the total phenol content of *E. stolonifera* hydrolysate, surpassing both reaction temperature and reaction time. With an increase in the solid-to-liquid ratio during the reaction, the total phenol content also increased.

2) The model predicted the optimum extraction conditions for the total phenol content of hydrolyzed *E. stolonifera* to be an extraction temperature of 198.5℃, an extraction time of 36.21 min, and a solid-to-liquid ratio of 12.23 (g/mL). These conditions resulted in a total phenol content of 53.93 mg PG/g, which was confirmed as the response value.

3) Ethanol extraction was conducted to compare with the extract obtained using optimum extraction conditions for *E. stolonifera*. The extract obtained under optimum extraction conditions exhibited $ABTS^{+}$, DPPH radical scavenging ability, and FRAP

activity of 70.94 ± 0.15, 60.03 ± 0.35, and 29.45 ± 0.39 mg trolox equivalent/g dried sample, respectively.

4) The total phenolic content and total flavonoid content of the extract under optimum extraction conditions were determined as 50.01 ± 0.12 and 43.58 ± 0.01, respectively. As total phenolic content and total polyphenolic content have a strong correlation with antioxidant activity, we examined the correlation between the total phenolic content and total flavonoid content of the optimized extracts and their antioxidant activity. There was a strong correlation found between the DPPH radical scavenging capacity and ferric ion reducing power (R^2=0.997), as well as the $ABTS^+$ radical scavenging capacity and total flavonoid content (R^2=0.901). The correlation analysis demonstrated a notable relationship between total phenolic content and antioxidant activity.

5) Furthermore, an analysis of phenolic compounds in the extract of *E. stolonifera* under optimum extraction conditions revealed the presence of 4-hydroxybenzoic acid, gallic acid, rutin, chlorogenic acid, and 4-hydroxy-3,5-dimethoxycinnamic acid in amounts of 1674.89 ± 0.08, 135.64 ± 0.07, 674.95 ± 0.15, 704.88 ± 1.09, and 114.06 ± 0.09 μg/g, respectively.

6) The antihypertensive activity of the optimal condition extract of *E. stolonifera* was measured using captopril (1%) as a standard, which is primarily used to treat hypertension. The extract showed 95.87±0.01% activity.

7) In the assessment of anti-diabetic activity, 1% acarbose was used as the standard substance, with the optimal extract of *E. stolonifera* exhibiting a noteworthy activity of 69.29% ± 1.83%. The IC_{50} value for the optimal extract of *E. stolonifera* was 7.17 ± 0.05 μg/mL.

8) Diclofenac sodium (1%) was employed as a standard substance to assess anti-inflammatory activity, with the optimal extract of *E. stolonifera* exhibiting an activity of 68.55% ± 0.98%.

9) The extract obtained under optimum extraction conditions was subjected to freeze-drying and its structural properties were analyzed using XRD and FT-IR. Comparisons revealed the presence of both KCl and NaCl in both the optimal extract powder and the raw material. Molecular structure analysis through FT-IR indicated the presence of molecular structures such as O-H groups and C-H groups.

Therefore, this study obtained the hydrolysate of *E. stolonifera* through the subcritical water extraction process. This method is not only safe and cost-effective but also allows for the utilization of functional substances in food. The optimal extraction conditions for the total phenolic content were established using the reaction surface analysis method to confirm the physicochemical and physiological activities. It can be concluded that *E. stolonifera* can be highly utilized as a basic material for the development of functional food, medicine, and cosmetic materials.

V. References

Admassu, H., Gasmalla, M. A. A., Yang, R., & Zhao, W. (2018). Bioactive peptides derived from seaweed protein and their health benefits: antihypertensive, antioxidant and antidiabetic properties. *Journal of Food Science*, 83(1), 6-16.

Alhajabdalla, M., Mahmoud, H., Nasser, M. S., Hussein, I. A., Ahmed, R., & Karami, H. (2021). Application of response surface methodology and box–behnken design for the optimization of the stability of fibrous dispersion used in drilling and completion operations. *ACS omega*, 6(4), 2513-2525.

Ali, L., Khan, S., Nazir, M., Raiz, N., Naz, S., Zengin, G., Mukhtar, M., Parveen, S., Shazmeen, N., Saleem, M., & Tareen, R. B. (2021). Chemical profiling, in vitro biological activities and Pearson correlation between phenolic contents and antioxidant activities of Caragana brachyantha Rech. f. *South African Journal of Botany*, 140, 189-193.

AOAC (2000). Methods of analysis of AOAC International. AOAC International, Maryland, USA.

Asl, A. H., & Khajenoori, M. (2013). Subcritical water extraction. *Mass Transfer-Advances in sustainable energy and environment oriented numerical modeling*, 459-487.

Banerjee, G., & Chattopadhyay, P. (2019). Vanillin biotechnology: the perspectives and future. *Journal of the Science of Food and Agriculture*, 99(2), 499-506.

Belda, M., Sanchez, D., Bover, E., Prieto, B., Padrón, C., Cejalvo, D., & Lloris, J. M. (2016). Extraction of polyphenols in Himanthalia elongata and determination by high performance liquid chromatography with diode array detector prior to its potential use against oxidative stress. *Journal of Chromatography B*, 1033, 334-341.

Bezerra, M. A., Santelli, R. E., Oliveira, E. P., Villar, L. S., & Escaleira, L. A. (2008). Response surface methodology (RSM) as a tool for optimization in analytical chemistry. *Talanta*, 76(5), 965-977.

Boakye, P., Sewu, D. D., & Woo, S. H. (2018). Effect of thermal pretreatment on the extraction of potassium salt from alga Saccharina japonica. Journal of Analytical and Applied Pyrolysis, 133, 68-75

Boonchum, W., Peerapornpisal, Y., Kanjanapothi, D., Pekkoh, J., Pumas, C., Jamjai, U., Amornlerdpison, D., Noiraksar, T., & Vacharapiyasophon, P. (2011). Antioxidant activity of some seaweed from the Gulf of Thailand. *International Journal of Agriculture and Biology*, 13(1), 95-99.

Cao, B., Yuan, J., Jiang, D., Wang, S., Barati, B., Hu, Y., Yuan, C., Gong, X., & Wang, Q. (2021). Seaweed-derived biochar with multiple active sites as a heterogeneous catalyst for converting macroalgae into acid-free biooil containing abundant ester and sugar substances. *Fuel*, 285, 119164.

Cerretani, L., & Bendini, A. (2010). Rapid assays to evaluate the antioxidant capacity of phenols in virgin olive oil. *In Olives and olive oil in health and disease prevention*, 67, 625-635.

Chamika, W. A. S., Ho, T. C., Roy, V. C., Kiddane, A. T., Park, J. S., Kim, G. D., & Chun, B. S. (2021). In vitro characterization of bioactive compounds extracted from sea urchin (*Stomopneustes variolaris*) using green and conventional techniques. *Food Chemistry*, 361, 129866.

Chen, R., Qi, Q. L., Wang, M. T., & Li, Q. Y. (2016). Therapeutic potential of naringin: an overview. *Pharmaceutical biology*, 54(12), 3203-3210.

Cheng, Y., Xue, F., Yu, S., Du, S., & Yang, Y. (2021). Subcritical water extraction of natural products. *Molecules*, 26(13), 4004.

Čmiková, N., Galovičová, L., Miškeje, M., Borotová, P., Kluz, M., & Kačániová, M. (2022). Determination of antioxidant, antimicrobial activity, heavy metals and elements content of seaweed extracts. *Plants*, 11(11), 1493.

Cotas, J., Leandro, A., Monteiro, P., Pacheco, D., Figueirinha, A., Gonçalves, A. M., Silva, G. J. D., & Pereira, L. (2020). Seaweed phenolics: From extraction to applications. *Marine drugs*, 18(8), 384.

Dawczynski, C., Schubert, R., & Jahreis, G. (2007). Amino acids, fatty acids, and dietary fibre in edible seaweed products. *Food chemistry*, 103(3), 891-899.

Dowarah, J., & Singh, V. P. (2020). Anti-diabetic drugs recent approaches and advancements. *Bioorganic & medicinal chemistry*, 28(5), 115263.

Farasat, M., Khavari-Nejad, R. A., Nabavi, S. M. B., & Namjooyan, F. (2014). Antioxidant activity, total phenolics and flavonoid contents of some edible green seaweeds from northern coasts of the Persian Gulf. *Iranian journal of pharmaceutical research*: IJPR, 13(1), 163-170.

Filinchuk, Y., Cerny, R., & Hagemann, H. (2009). Insight into Mg $(BH_4)_2$ with synchrotron X-ray diffraction: structure revision, crystal chemistry, and anomalous thermal expansion. *Chemistry of Materials*, 21(5), 925-933.

Ganeshpurkar, A., & Saluja, A. (2020). The pharmacological potential of catechin. *Indian Journal of Biochemistry and Biophysics (IJBB)*, 57(5), 505-511.

Gao, D., Kobayashi, T., & Adachi, S. (2014). Kinetics of sucrose hydrolysis in a subcritical water-ethanol mixture. *Journal of Applied Glycoscience*, 61(1), 9-13.

Garcia, E. J., Oldoni, T. L. C., Alencar, S. M. D., Reis, A., Loguercio, A. D., & Grande, R. H. M. (2012). Antioxidant activity by DPPH assay of potential solutions to be applied on bleached teeth. *Brazilian dental journal*, 23, 22-27.

Gbashi, S., Adebo, O. A., Piater, L., Madala, N. E., & Njobeh, P. B. (2017). Subcritical water extraction of biological materials. *Separation & Purification Reviews*, 46(1), 21-34.

Gereniu, C. R. N., Saravana, P. S., Getachew, A. T., & Chun, B. S. (2017). Characteristics of functional materials recovered from Solomon Islands red seaweed (*Kappaphycus alvarezii*) using pressurized hot water extraction. *Journal of Applied Phycology*, 29, 1609-1621.

Getachew, A. T., & Chun, B. S. (2017). Influence of pretreatment and modifiers on subcritical water liquefaction of spent coffee grounds: A green waste valorization approach. *Journal of cleaner production*, 142, 3719-3727.

Ghani, U. (2015). Re-exploring promising α-glucosidase inhibitors for potential development into oral anti-diabetic drugs: Finding needle in the haystack. *European journal of medicinal chemistry*, 103, 133-162.

Haidar, Z., Fatema, K., Shoily, S. S., & Sajib, A. A. (2023). Disease-associated metabolic pathways affected by heavy metals and metalloid. *Toxicology Reports*, 10, 554-570.

Hakim, M. M., & Patel, I. C. (2020). A review on phytoconstituents of marine brown algae. *Future Journal of Pharmaceutical Sciences*, 6, 1-11.

Han, X., Kim, W. H., Choi, S. I., Men, X., Lee, S. J., Jin, H. G., Oh, H. J., Kang, D. H., Lee, B. Y., & Lee, O. H. (2021). Antioxidant and anti-cholesterol activities of standardized *Ecklonia stolonifera* Extract. *Journal of Food Hygiene and Safety*, 36(4), 353-362.

Haq, M., Ahmed, R., Cho, Y. J., & Chun, B. S. (2017). Quality properties and biopotentiality of edible oils from Atlantic salmon by-products extracted by supercritial carbon dioxide and conventional methods. *Waste and Biomass Valorization*, 8, 1953-1967.

Haque, A. R., Park, J. S., Ho, T. C., Roy, V. C., Ali, M. S., Kiddane, A. T., Kim, G. D., & Chun, B. S. (2023). Characterization of oil and amino acids obtained from yellow corvina by-products using subcritical and supercritical fluids. *The Journal of Supercritical Fluids*, 199, 105970.

Ho, T. C., Lim, J. S., Kim, S. J., Kim, S. Y., & Chun, B. S. (2023). In Vitro Biodegradation, Drug Absorption, and Physical Properties of Gelatin-Fucoidan Microspheres Made of Subcritical-Water-Modified Fish Gelatin. *Marine Drugs*, 21(5), 287.

Holdt, S. L., & Kraan, S. (2011). Bioactive compounds in seaweed: functional food applications and legislation. *Journal of applied phycology*, 23, 543-597.

Imani, A., Maleki, N., Bohlouli, S., Kouhsoltani, M., Sharifi, S., & Maleki Dizaj, S. (2021). Molecular mechanisms of anticancer effect of rutin. *Phytotherapy Research*, 35(5), 2500-2513.

Isemura, M. (2019). Catechin in human health and disease. *Molecules*, 24(3), 528.

Joe, M. J., Kim, S. N., Choi, H. Y., Shin, W. S., Park, G. M., Kang, D. W., & Kim, Y. K. (2006). The inhibitory effects of eckol and dieckol from *Ecklonia stolonifera* on the expression of matrix metalloproteinase-1 in human dermal fibroblasts. *Biological and Pharmaceutical Bulletin*, 29(8), 1735-1739.

Jung, H. A., Hyun, S. K., Kim, H. R., & Choi, J. S. (2006). Angiotensin-converting enzyme I inhibitory activity of phlorotannins from *Ecklonia stolonifera*. *Fisheries Science*, 72, 1292-1299.

Jung, H. A., Islam, M. N., Lee, C. M., Oh, S. H., Lee, S., Jung, J. H., & Choi, J. S. (2013). Kinetics and molecular docking studies of an anti-diabetic complication inhibitor fucosterol from edible brown algae *Eisenia bicyclis* and *Ecklonia stolonifera*. *Chemico-biological interactions*, 206(1), 55-62.

Jung, H. A., Jung, H. J., Jeong, H. Y., Kwon, H. J., Ali, M. Y., & Choi, J. S. (2014a). Phlorotannins isolated from the edible brown alga *Ecklonia stolonifera* exert anti-adipogenic activity on 3T3-L1 adipocytes by downregulating C/EBPα and PPARγ. *Fitoterapia*, 92, 260-269.

Jung, H. A., Kim, J. I., Choung, S. Y., & Choi, J. S. (2014b). Protective effect of the edible brown alga *Ecklonia stolonifera* on doxorubicin-induced hepatotoxicity in primary rat hepatocytes. *Journal of Pharmacy and Pharmacology*, 66(8), 1180-1188.

K., Gereniu, C. R. N., Chae, S. J., Kang, H. W., Woo, H. C., & Chun, B. S. (2019). Ultrasound-mediated fucoxanthin rich oil nanoemulsions stabilized by κ-carrageenan: Process optimization, bio-accessibility and cytotoxicity. *Ultrasonics Sonochemistry*, 55, 105-116.

Kahkeshani, N., Farzaei, F., Fotouhi, M., Alavi, S. S., Bahramsoltani, R., Naseri, R., Momtaz, S., Abbasabadi, Z., Rahimi, R., Farzaei, M. H., & Bishayee, A. (2019). Pharmacological effects of gallic acid in health and diseases: A mechanistic review. *Iranian journal of basic medical sciences*, 22(3), 225.

Kang, H. S., Chung, H. Y., Jung, J. H., Son, B. W., & Choi, J. S. (2003). A new phlorotannin from the brown alga *Ecklonia stolonifera*. *Chemical and pharmaceutical bulletin*, 51(8), 1012-1014.

Kang, H. S., Chung, H. Y., Kim, J. Y., Son, B. W., Jung, H. A., & Choi, J. S. (2004). Inhibitory phlorotannins from the edible brown alga *Ecklonia stolonifera* on total reactive oxygen species (ROS) generation. *Archives of pharmacal research*, 27, 194-198.

Khan, F., Jeong, G. J., Khan, M. S. A., Tabassum, N., & Kim, Y. M. (2022). Seaweed-Derived phlorotannins: A review of multiple biological roles and action mechanisms. *Marine Drugs*, 20(6), 384.

Khan, H., Yerramilli, A. S., D'Oliveira, A., Alford, T. L., Boffito, D. C., & Patience, G. S. (2020). Experimental methods in chemical engineering: X-ray diffraction spectroscopy-XRD. *The Canadian journal of chemical engineering*, 98(6), 1255-1266.

Kim, A. R., Shin, T. S., Lee, M. S., Park, J. Y., Park, K. E., Yoon, N. Y., Kim, J. S., Choi, J. S., Jang, B. C., Byun, D. S., Park, N. K., & Kim, H. R. (2009). Isolation and identification of phlorotannins from *Ecklonia stolonifera* with antioxidant and anti-inflammatory properties. *Journal of agricultural and food chemistry*, 57(9), 3483-3489.

Kim, S. Y., Roy, V. C., Park, J. S., & Chun, B. S. (2023). Extraction and characterization of bioactive compounds from brown seaweed (*Undaria pinnatifida*) sporophyll using two sequential green extraction techniques. *Algal Research*, 103330.

Kuda, T., Kunii, T., Goto, H., Suzuki, T., & Yano, T. (2007). Varieties of antioxidant and antibacterial properties of *Ecklonia stolonifera* and *Ecklonia kurome* products harvested and processed in the Noto peninsula, Japan. *Food chemistry*, 103(3), 900-905.

Leal, D., Matsuhiro, B., Rossi, M., & Caruso, F. (2008). FT-IR spectra of alginic acid block fractions in three species of brown seaweeds. *Carbohydrate research*, 343(2), 308-316.

Lee, J. M., Ko, M. J., & Chung, M. S. (2015). Physicochemical properties and composition of ginsenosides in red ginseng extract as revealed by subcritical water extraction. *Korean Journal of Food Science and Technology*, 47(6), 757-764.

Lee, M. S., Kwon, M. S., Choi, J. W., Shin, T., No, H. K., Choi, J. S., Byun, D. S., Kim, J. I., & Kim, H. R. (2012). Anti-inflammatory activities of an ethanol extract of *Ecklonia stolonifera* in lipopolysaccharide-stimulated RAW 264.7 murine macrophage cells. *Journal of agricultural and food chemistry*, 60(36), 9120-9129.

Leelaprakash, G., & Dass, S. M. (2011). Invitro anti-inflammatory activity of methanol extract of *Enicostemma axillare*. *International Journal of Drug Development and Research*, 3(3), 189-196.

Li, Y. X., Wijesekara, I., Li, Y., & Kim, S. K. (2011). Phlorotannins as bioactive agents from brown algae. *Process biochemistry*, 46(12), 2219-2224.

Liu, C. C., Zhao, G. L., Li, Y. N., Ding, Z. P., Liu, Q. G., & Li, J. L. (2011). Contribution of phenolics and flavonoids to anti-oxidat activity and of ethanol extract from *Eichharnia crassipes*. *Advanced Materials Research*, 156, 1372-1377.

Lordan, S., Smyth, T. J., Soler-Vila, A., Stanton, C., & Ross, R. P. (2013). The α-amylase and α-glucosidase inhibitory effects of Irish seaweed extracts. *Food chemistry*, 141(3), 2170-2176.

Lou, H., Li, W., Li, C., & Wang, X. (2013). Systematic investigation on parameters of solution blown micro/nanofibers using response surface methodology based on box-Behnken design. *Journal of Applied Polymer Science*, 130(2), 1383-1391.

Men, X., Han, X., Lee, S. J., Oh, G., Jin, H., Oh, H. J., Kim, E. J., Kim, J. W., Lee, B. Y., Choi, S. I., & Lee, O. H. (2022). In-depth understanding of *Ecklonia stolonifera* okamura: A review of its bioactivities and bioactive compounds. *Marine Drugs*, 20(10), 607.

Meng, W., Mu, T., Sun, H., & Garcia-Vaquero, M. (2021). Phlorotannins: A review of extraction methods, structural characteristics, bioactivities, bioavailability, and future trends. *Algal Research*, 60, 102484.

Moon, S. K., (2005). Analysis of total sugar by extraction condition and material to develope the extraction process of ginseng polysaccharide. *Korean Journal of Food Preservation*, 12(4), 367-371.

Nagayama, K., Iwamura, Y., Shibata, T., Hirayama, I., & Nakamura, T. (2002). Bactericidal activity of phlorotannins from the brown alga *Ecklonia kurome*. *Journal of Antimicrobial Chemotherapy*, 50(6), 889-893.

Nair, D., Vanuopadath, M., Balasubramanian, A., Iyer, A., Ganesh, S., Anil, A. N., Vikraman, V., Pillai, P., Bose, C., Nair, B. G., Pai, J. G., & Nair, S. S. (2019). Phlorotannins from *Padina tetrastromatica*: Structural characterisation and functional studies. *Journal of Applied Phycology*, 31(5), 3131-3141.

National Institute of Fisheries Science (NIFS). (2023). Species information. Retrieved from: https://www.nifs.go.kr/frcenter/sub/sub_view.html?taxonId=134855

Naveed, M., Hejazi, V., Abbas, M., Kamboh, A. A., Khan, G. J., Shumzaid, M., Ahmad, F., Babazadeh, D., FangFang, X., Modarresi-Ghazani, F., WenHua, L., & XiaoHui, Z. (2018). Chlorogenic acid (CGA): A pharmacological review and call for further research. *Biomedicine & pharmacotherapy*, 97, 67-74.

Nićiforović, N., & Abramovič, H. (2014). Sinapic acid and its derivatives: natural sources and bioactivity. *Comprehensive reviews in food science and food safety*, 13(1), 34-51.

Nunes, S. C., Pereira, R. F., Sousa, N., Silva, M. M., Almeida, P., Figueiredo, F. M., & de Zea Bermudez, V. (2017). Eco-Friendly Red Seaweed-Derived Electrolytes for Electrochemical Devices. *Advanced Sustainable Systems*, 1(9), 1700070.

O'sullivan, A. M., O'callaghan, Y. C., O'grady, M. N., Queguineur, B., Hanniffy, D., Troy, D. J., Kerry, J. P., & O'brien, N. M. (2011). In vitro and cellular antioxidant activities of seaweed extracts prepared from five brown seaweeds harvested in spring from the west coast of Ireland. *Food chemistry*, 126(3), 1064-1070.

Owoyele, V. B., Adediji, J. O., & Soladoye, A. O. (2005). Anti-inflammatory activity of aqueous leaf extract of Chromolaena odorata. *Inflammopharmacology*, 13, 479-484.

Oyinade, A., Kovo, A. S., & Hill, P. (2016). Synthesis, characterization and ion exchange isotherm of zeolite Y using Box-Behnken design. *Advanced Powder Technology*, 27(2), 750-755.

Pangestuti, R., Haq, M., Rahmadi, P., & Chun, B. S. (2021). Nutritional value and biofunctionalities of two edible green seaweeds (*Ulva lactuca* and *Caulerpa racemosa*) from Indonesia by subcritical water hydrolysis. *Marine Drugs*, 19(10), 578.

Park, J. S., Han, J. M., Shin, Y. N., Park, Y. S., Shin, Y. R., Park, S. W., Roy, V. C., Lee, H. J., Kumagai, Y., Kishimura, H., & Chun, B. S. (2023a). Exploring Bioactive Compounds in Brown Seaweeds Using Subcritical Water: A Comprehensive Analysis. *Marine Drugs*, 21(6), 328.

Park, J. S., Han, J. M., Surendhiran, D., & Chun, B. S. (2022). Physicochemical and biofunctional properties of *Sargassum thunbergii* extracts obtained from subcritical water extraction and conventional solvent extraction. *The Journal of Supercritical Fluids*, 182, 105535.

Park, J. S., Jeong, Y. R., & Chun, B. S. (2019). Physiological activities and bioactive compound from laver (*Pyropia yezoensis*) hydrolysates by using subcritical water hydrolysis. *The Journal of Supercritical Fluids*, 148, 130-136.

Park, J. Y., Kim, J. H., Kwon, J. M., Kwon, H. J., Jeong, H. J., Kim, Y. M., Kim, D., Lee, W. S., & Ryu, Y. B. (2013). Dieckol, a SARS-CoV 3CLpro inhibitor, isolated from the edible brown algae *Ecklonia cava*. *Bioorganic & medicinal chemistry*, 21(13), 3730.

Park, Y. S., Roy, V. C., Park, J. S., Han, J. M., Shin, Y. N., Shin, Y. R., Park, S. W., & Chun, B. S. (2023b). Bioactive compounds obtained via subcritical water hydrolysis of *Ecklonia stolonifera*: Characterization and potential application. *Journal of Applied Phycology*, 1-9.

Pérez, M. J., Falqué, E., & Domínguez, H. (2016). Antimicrobial action of compounds from marine seaweed. *Marine drugs*, 14(3), 52.

Pinteus, S., Silva, J., Alves, C., Horta, A., Fino, N., Rodrigues, A. I., Mendes, S., & Pedrosa, R. (2017). Cytoprotective effect of seaweeds with high antioxidant activity from the Peniche coast (Portugal). *Food chemistry*, 218, 591-599.

Plaza, M., Abrahamsson, V., & Turner, C. (2013). Extraction and neoformation of antioxidant compounds by pressurized hot water extraction from apple byproducts. *Journal of agricultural and food chemistry*, 61(23), 5500-5510.

Rajauria, G. (2018). Optimization and validation of reverse phase HPLC method for qualitative and quantitative assessment of polyphenols in seaweed. *Journal of pharmaceutical and biomedical analysis*, 148, 230-237.

Rajeswari, R., & Jeyaprakash, K. (2019). Bioactive potential analysis of brown seaweed *Sargassum wightii* using UV-VIS and FT-IR. *Journal of Drug Delivery and Therapeutics*, 9(1), 150-153.

Ren, D., Noda, H., Amano, H., Nishino, T., & Nishizawa, K. (1994). Study on antihypertensive and antihyperlipidemic effects of marine algae. *Fisheries science*, 60(1), 83-88.

Ryu, B., Li, Y., Qian, Z. J., Kim, M. M., & Kim, S. K. (2009). Differentiation of human osteosarcoma cells by isolated phlorotannins is subtly linked to COX-2, iNOS, MMPs, and MAPK signaling: Implication for chronic articular disease. *Chemico-biological interactions*, 179(2-3), 192-201.

Sansone, C., Brunet, C., Noonan, D. M., & Albini, A. (2020). Marine algal antioxidants as potential vectors for controlling viral diseases. *Antioxidants*, 9(5), 392.

Saqib, A. A. N., & Whitney, P. J. (2011). Differential behaviour of the dinitrosalicylic acid (DNS) reagent towards mono-and di-saccharide sugars. *Biomass and bioenergy*, 35(11), 4748-4750.

Saravana, P. S., Cho, Y. N., Woo, H. C., & Chun, B. S. (2018). Green and efficient extraction of polysaccharides from brown seaweed by adding deep eutectic solvent in subcritical water hydrolysis. *Journal of Cleaner Production*, 198, 1474-1484.

Saravana, P. S., Choi, J. H., Park, Y. B., Woo, H. C., & Chun, B. S. (2016). Evaluation of the chemical composition of brown seaweed (*Saccharina japonica*) hydrolysate by pressurized hot water extraction. *Algal Research*, 13, 246-254.

Saravana, P. S., Shanmugapriya, K., Gereniu, C. R. N., Chae, S. J., Kang, H. W., Woo, H. C., & Chun, B. S. (2019). Ultrasound-mediated fucoxanthin rich oil nanoemulsions stabilized by κ-carrageenan: Process optimization, bio-accessibility and cytotoxicity. *Ultrasonics Sonochemistry*, 55, 105-116.

Sasaki, M., Kabyemela, B., Malaluan, R., Hirose, S., Takeda, N., Adschiri, T., & Arai, K. (1998). Cellulose hydrolysis in subcritical and supercritical water. *The Journal of Supercritical Fluids*, 13(1-3), 261-268.

Seca, A. M., & Pinto, D. C. (2018). Overview on the antihypertensive and anti-obesity effects of secondary metabolites from seaweeds. *Marine drugs*, 16(7), 237.

Shrestha, S., Zhang, W., & Smid, S. D. (2021). Phlorotannins: A review on biosynthesis, chemistry and bioactivity. *Food Bioscience*, 39, 100832.

Singh, B. N., Shankar, S., & Srivastava, R. K. (2011). Green tea catechin, epigallocatechin-3-gallate (EGCG): mechanisms, perspectives and clinical applications. *Biochemical pharmacology*, 82(12), 1807-1821.

Viganó, J., Brumer, I. Z., de Campos Braga, P. A., da Silva, J. K., Júnior, M. R. M., Reyes, F. G. R., & Martínez, J. (2016). Pressurized liquids extraction as an alternative process to readily obtain bioactive compounds from passion fruit rinds. *Food and Bioproducts Processing*, 100, 382-390.

Walton, N. J., Mayer, M. J., & Narbad, A. (2003). Vanillin. *Phytochemistry*, 63(5), 505-515.

Wan, C. W., Wong, C. N. Y., Pin, W. K., Wong, M. H. Y., Kwok, C. Y., Chan, R. Y. K., Yu, P. H. F., & Chan, S. W. (2013). Chlorogenic acid exhibits cholesterol lowering and fatty liver attenuating properties by up-regulating the gene expression of PPAR-α in hypercholesterolemic rats induced with a high-cholesterol diet. *Phytotherapy Research*, 27(4), 545-551.

Wang, S., Bilal, M., Hu, H., Wang, W., & Zhang, X. (2018). 4-Hydroxybenzoic acid-a versatile platform intermediate for value-added compounds. *Applied microbiology and biotechnology*, 102, 3561-3571.

Wang, S., Jiang, X. M., Han, X. X., & Wang, H. (2008). Fusion characteristic study on seaweed biomass ash. *Energy & fuels*, 22(4), 2229-2235.

Wang, X., Deng, Y., Xie, P., Liu, L., Zhang, C., Cheng, J., Zhang, Y., Liu, Y., Huang, L., & Jiang, J. (2023). Novel bioactive peptides from Ginkgo biloba seed protein and evaluation of their α-glucosidase inhibition activity. *Food Chemistry*, 404, 134481.

Wei, D., Fan, W., & Xu, Y. (2019). In vitro production and identification of angiotensin converting enzyme (ACE) inhibitory peptides derived from distilled spent grain prolamin isolate. *Foods*, 8(9), 390.

Wei, R., Lee, M. S., Lee, B., Oh, C. W., Choi, C. G., & Kim, H. R. (2016). Isolation and identification of anti-inflammatory compounds from ethyl acetate fraction of

Ecklonia stolonifera and their anti-inflammatory action. *Journal of Applied Phycology*, 28, 3535-3545.

Yoon, J. S., Yadunandam, A. K., Kim, S. J., Woo, H. C., Kim, H. R., & Kim, G. D. (2013). Dieckol, isolated from *Ecklonia stolonifera*, induces apoptosis in human hepatocellular carcinoma Hep3B cells. *Journal of natural medicines*, 67, 519-527.

Yoon, N. Y., Chung, H. Y., Kim, H. R., & Choi, J. E. (2008). Acetyl-and butyrylcholinesterase inhibitory activities of sterols and phlorotannins from *Ecklonia stolonifera*. *Fisheries Science*, 74, 200-207.

Abstract (in Korean)

반응표면법에 의한 곰피(*Ecklonia stolonifera*) 아임계 수 추출물의 페놀 화합물 최적화

박 예 슬

국 립 부 경 대 학 교 대 학 원 식 품 공 학 과

요 약

곰피(*Ecklonia stolonifera*)는 다시마목 미역과에 속하는 해조류로 여러 연구에서 그 기능이 증명된 바 있다. 친환경 추출 기술인 아임계 수 가수분해법을 사용하여 *E. stolonifera*에서 생리 활성 화합물을 추출하였다. 가수분해의 반응 온도는 120℃에서 220℃ 사이였으며, 이는 당, 페놀, 플라보노이드 및 항산화제와 같은 활성 화합물의 방출에 중요한 역할을 하였다. 온도별 추출 결과 최적의 온도 조건은 195℃로 나타났기 때문에 Response surface methodology(RSM)의 중심온도를 195℃로 설정하여 온도는 160℃, 195℃, 230℃, 시간은 20분, 40분, 60분, 비율은 10 g/mL, 20 g/mL, 30 g/mL로 설정하였다. 추출 온도, 시간, 비율의 최적 조건은 198.50℃, 36.21분, 12.23 g/mL로 나타났다. 추출물 내의 개별 페놀 화합물을 식별하기 위해 고성능 액체 크로마토그래피(HPLC)를 사용해 분석한 결과, 곰피에는 페놀화합물 중 4-hydroxybenzoic acid, Chlorogenic acid, Rutin, Gallic acid, 4-hydroxy-3,5-dimethoxycinnamic acid가 우세하게 나타났다. 곰피의 아임계 수 추출물은 $ABTS^{+}$, DPPH, FRAP 등 다양한 분석에서 높은 항산화 활성을 나타내었다. 최적 조건에서의 추출물의 경우, $ABTS^{+}$ 값이 70.94 ± 0.15 mg trolox equivalent/g dried sample, DPPH값이 60.03 ± 0.35 mg trolox equivalent/g dried sample, FRAP값이 29.45 ± 0.39mg trolox equivalent/g dried sample으로 에탄올 추출물보다 높게 나타났다. 또한 *E. stolonifera*의 물리화학적 특성(TPC, TFC, TSC 및 RSC)을 분석한 결과, 최적조건 추출물의 경우 TPC값이 50.01 ± 0.12 mg phloroglucinol equivalent/g dried sample, TFC값이 43.58±0.01 mg quercetin equivalent/g dried sample로 에탄올 추출물의 총 페놀함량보다 약 3배 가량 높은 값을 나타내었다. TSC와 RSC 역시 각각 55.06 ± 1.51 mg glucose equivalent/g dried sample, 19.22 ± 0.23 mg glucose equivalent/g dried sample으로 에탄올 추출물보다 높게 나타났다. 구조적 특성(XRD, FT-IR)분석의 경우, 곰피 원물과의 비교도 함께 수행되었다. XRD 분석 결과, 원물에서는 KCl이 높게 나타났고, 최적조건

추출물과 에탄올 추출물에서는 NaCl이 주로 관찰되었다. FT-IR 분석 결과, 곰피 원물, 최적조건 추출물, 에탄올 추출물 모두에서 O-H기, C-H기, -C≡C-기, O-C-O기 및 C-O기가 관찰되었다. 또한, 항고혈압 활성을 평가한 결과, 양성 대조군으로 쓰인 1% captopril은 ≤99.22% ± 0.01%의 활성을 보였으며, *E. stolonifera* 가수분해물은 0.5%의 농도만으로 ≤95.87% ± 0.01%의 높은 활성을 보였다. 항당뇨 활성의 경우, 양성 대조군으로 쓰인 1% acarbose는 ≤96.68% ± 0.07%, *E. stolonifera* 가수분해물은 ≤69.29% ± 1.83%, 에탄올 추출물은 ≤92.67% ± 1.13%의 활성을 보였다. 항염증 활성을 확인한 결과, 1%의 diclofenac sodium이 양성대조군으로 사용되었으며, ≤66.80% ± 0.84%의 활성을 보였다. *E. stolonifera* 가수분해물은 ≤68.55% ± 0.98%, 에탄올 추출물은 ≤41.62% ± 0.66%의 활성을 나타내었다. 본 연구는 아임계 수 추출 방법을 이용해 *E. stolonifera* 추출물의 생리활성을 파악하였고, *E. stolonifera*는 기능성 식품 소재로서 잠재력을 확인하였다. *E. stolonifera* 추출물은 다양한 산업분야에 응용될 수 있을 것이다.